CHAPTER IV

RESULTS AND DISCUSSION

PART A: SYNTHESIS OF CATIONIC HYPERBRANCHED DENDRITIC POLYAMIDOAMINE

4.1 Synthesis of hyperbranched dendritic polyamidoamine

Hyperbranched dendritic polyamidoamine was synthesized according to Tomalia's well known method by repetitive reactions between Michael addition and amidation [42]. Michael addition reaction produced ester terminated products whereas amidation reaction produced amine terminated polymers. The reaction is shown in the Figure 4.1.

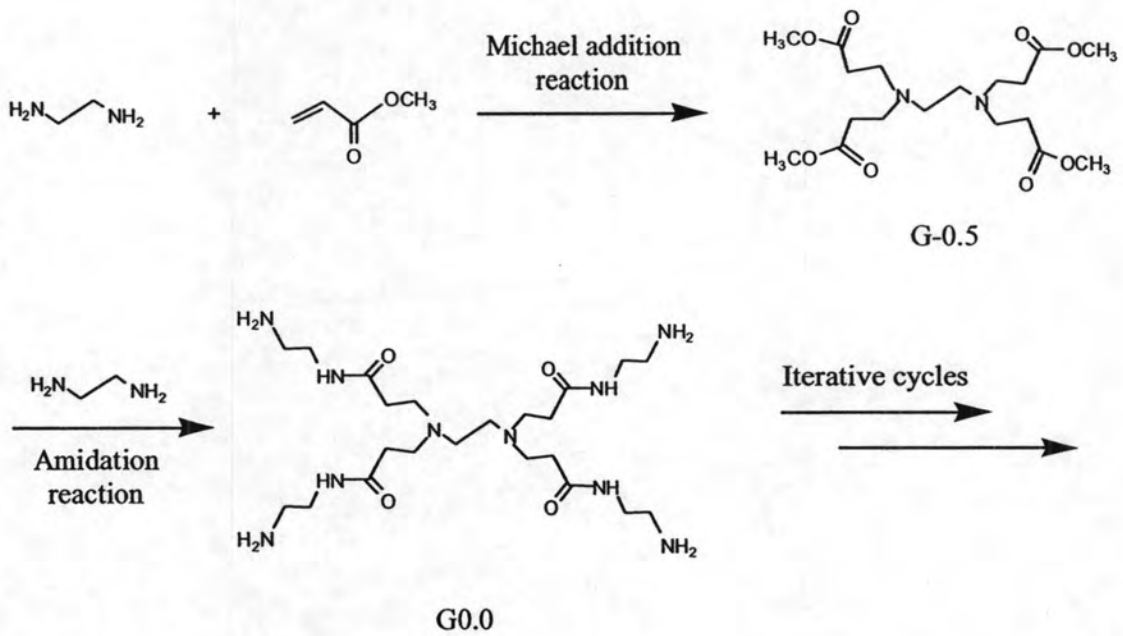

Figure 4.1 Synthesis of hyperbranched dendritic polyamidoamine

The synthesized hyperbranched PAMAM was characterized by FTIR and ^{1}H NMR spectroscopy.

4.1.1 FTIR Analysis

The hyperbranched PAMAM polymers obtained from repeating two processes, Michael addition (G-0.5, G 0.5 products) and amidation (G 0.0) were characterized using FTIR spectroscopy. FTIR results are shown in Figure 4.2.

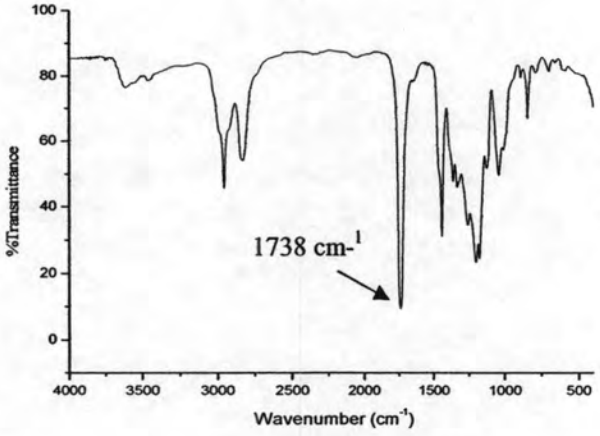

(a) G-0.5

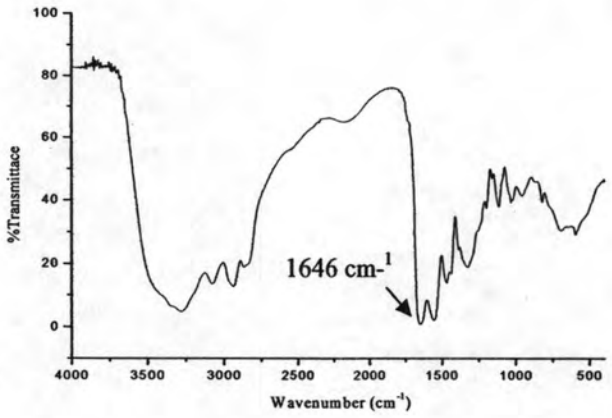

(b) G0.0

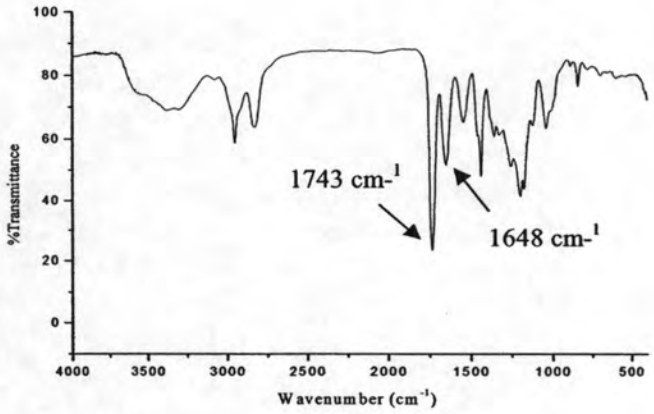

(c) G0.5

Figure 4.2 FTIR spectra of G-0.5 hyperbranched polyamidoamine (a), G0.0 hyperbranched polyamidoamine (b) and G0.5 hyperbranched polyamidoamine (c)

In Michael addition steps, the strong absorption band around 1740 cm^{-1} is observed, contributing to the methyl ester group. This peak completely disappears from the spectra of G0.0 as a result of the amidation reaction. In this step, the amide

linkage was formed, as observed the absorption band at 1646 cm^{-1}. Moreover, the terminal amine group was obtained which corresponds to the appearance of the strong absorption intensity of the N-H band in the region of 3000 - 3350 cm^{-1}. Its absorption intensity remarkably increases with an increase in PAMAM generation, reflecting that the number of terminal amine groups also significantly increases with an increase in synthesis rounds. It should be noted that the intensity of amine groups in the spectrum of G0.5 hyperbranched PAMAM significantly decreases as a result of the Michael addition which converted the amine group of G0.0 PAMAM to terminal methyl ester group.

4.1.2 ^{1}H NMR Analysis

^{1}H NMR analysis was also performed. The ^{1}H NMR spectrum of ester terminated PAMAM (G-0.5) is shown in Figure 4.3. The signal which indicates the presence of terminal methyl ester group (CH_3-O-) appears at ~3.26 ppm, corresponding to methyl proton of the methyl ester group. In this spectrum, the signal of amide proton is absent, indicating that the reaction of EDA with methyl ester end group could be prevented thanks to the presence of excessive amount of methanol (a suppressor of amidation reaction). The methyl ester signal completely disappears from the ^{1}H NMR spectrum of G0.0 due to the amidation reaction which resulted in the replacement of the methyl ester group by ethylene diamine. As a result, the amide bond was formed, as confirmed by the appearance of the signal of amide proton at around 7.75 ppm. In this study, methyl ester terminated hyperbranched PAMAM G-0.5 was achieved for being employed for the preparation of cationic hyperbranched PAMAM-ester.

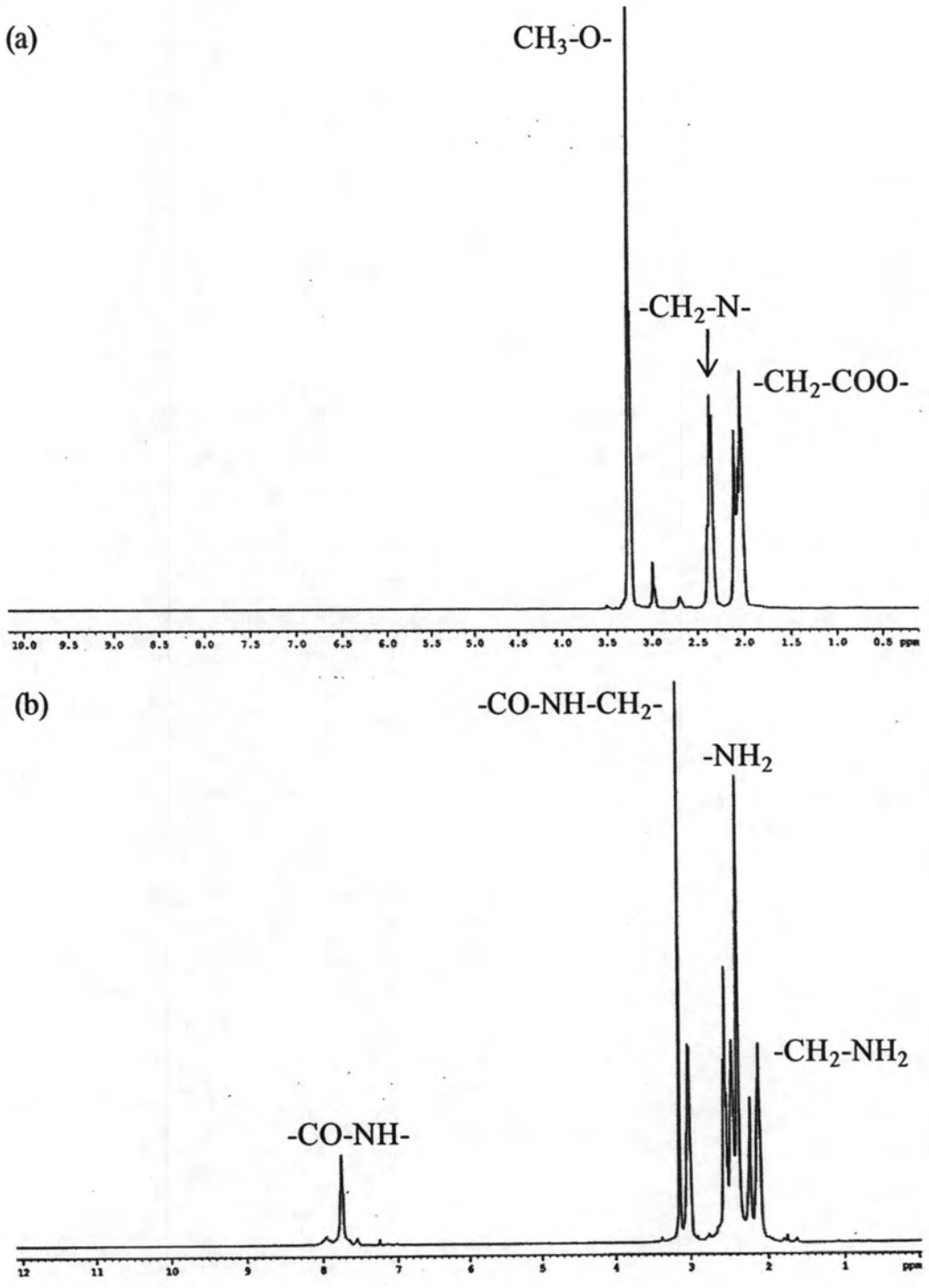

Figure 4.3 ^{1}H NMR spectra of G-0.5 hyperbranched PAMAM (a) and G0.0 hyperbranched PAMAM (b)

4.2 Synthesis of cationic hyperbranched dendritic polyamidoamine

The synthesized hyperbranched PAMAM was quaternized by using the methylation raction. The methylation of methyl ester terminated hyperbranched dendritic PAMAM (PAMAM-ester) with dimethyl sulphate is shown in Figure 4.4.

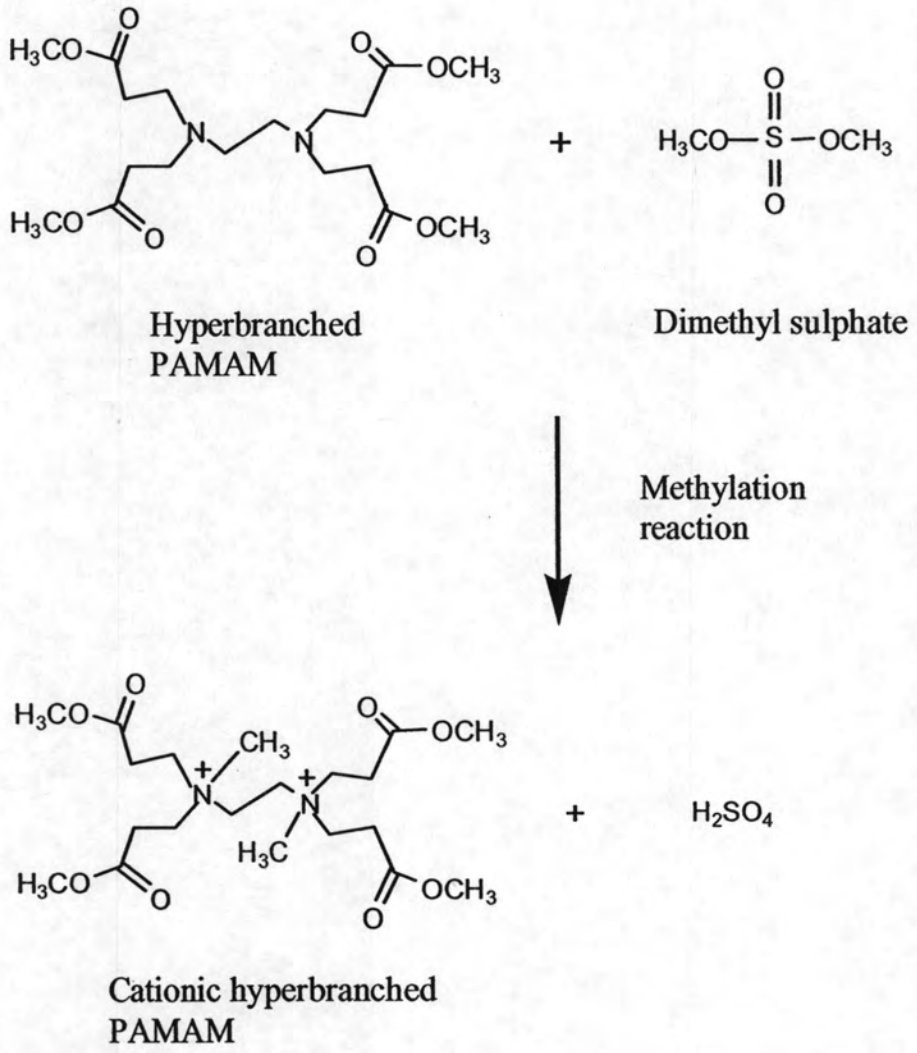

Figure 4.4 Methylation of methyl ester terminated hyperbranched dendritic PAMAM (PAMAM-ester, G-0.5) with dimethyl sulphate.

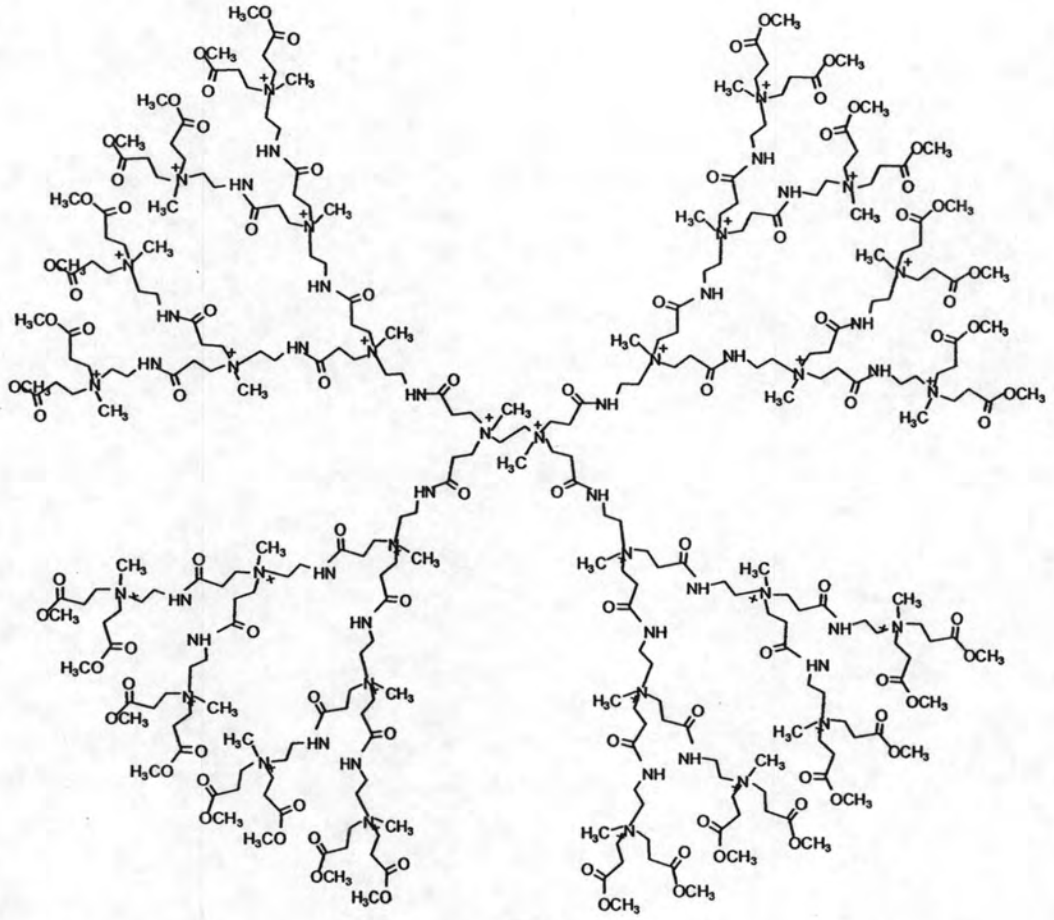

G2.5

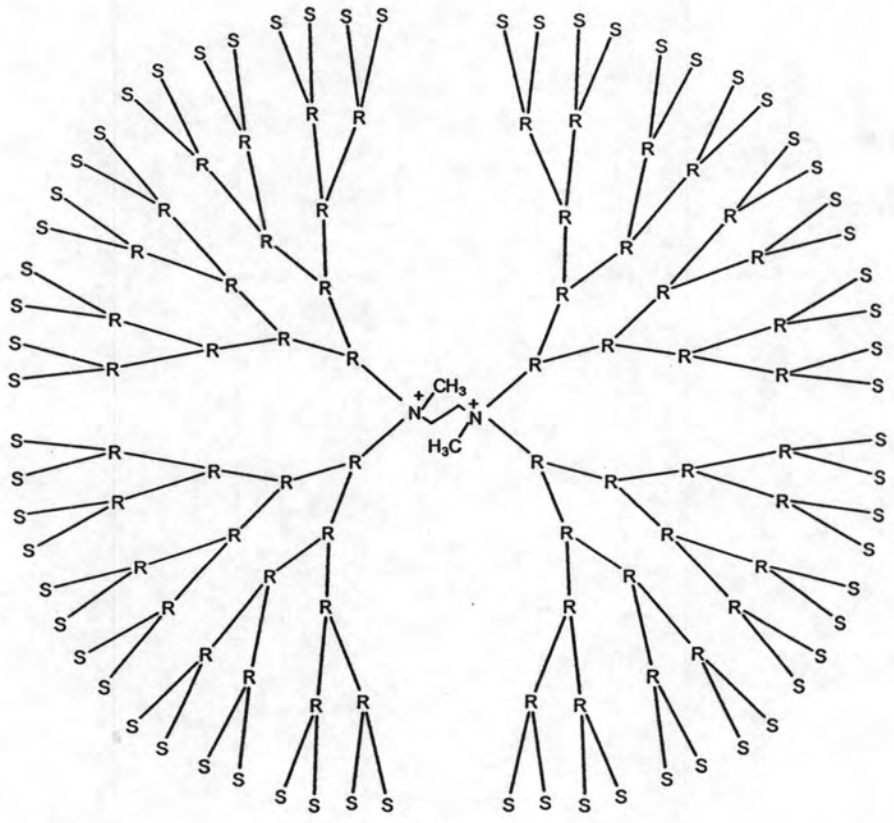

G3.5

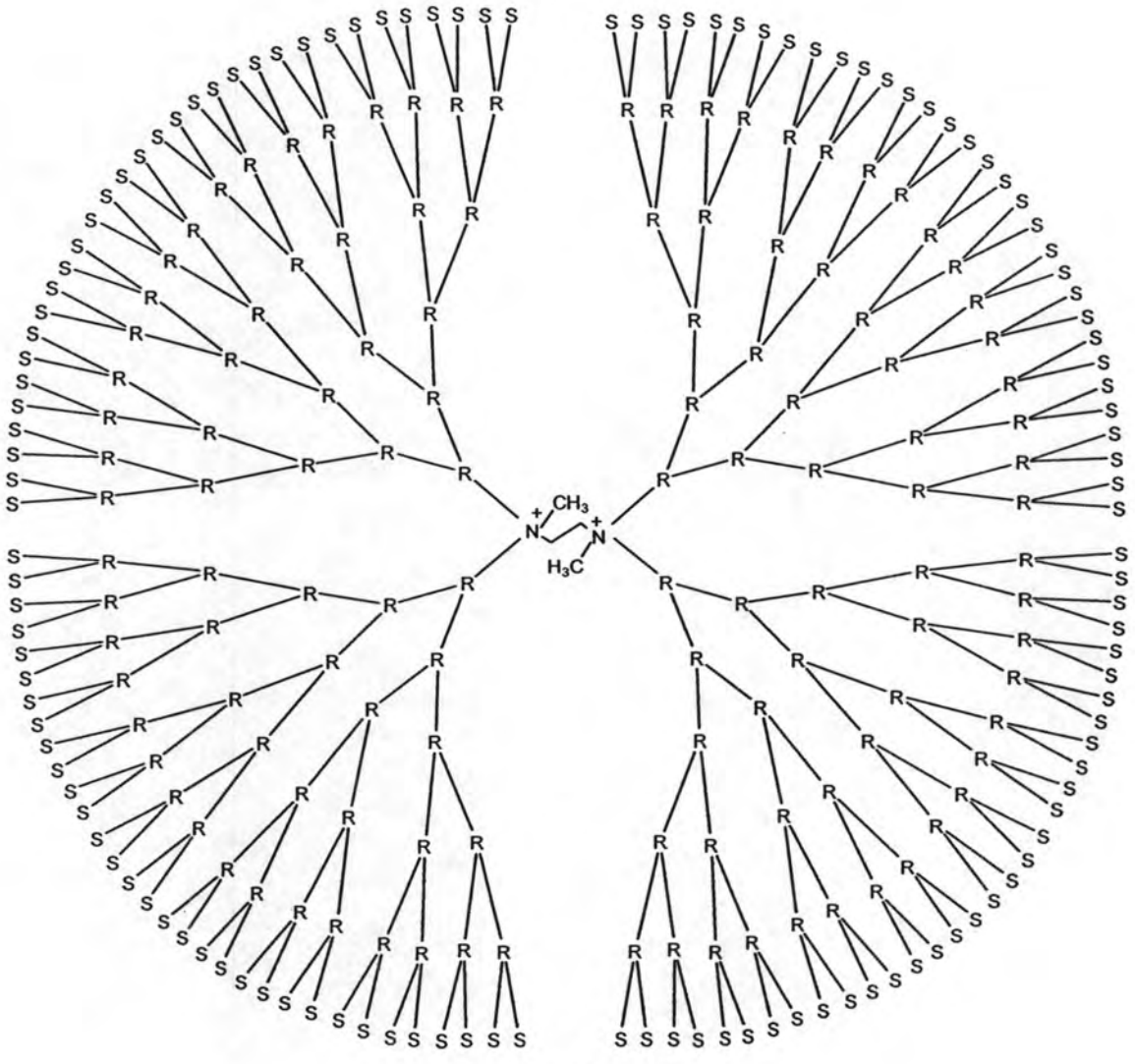

G4.5

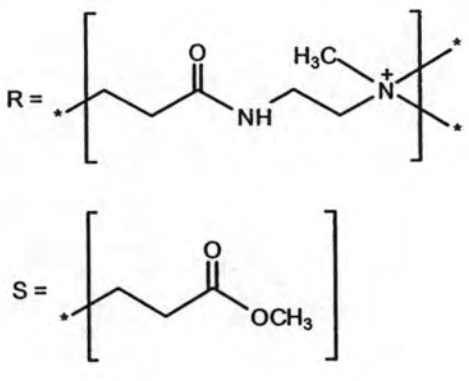

Figure 4.5 Structures of cationic hyperbranched PAMAM

The obtained cationic hyperbranched dendritic polyamidoamine was characterized by FTIR and ^{1}H NMR spectroscopy.

4.2.1 FTIR Analysis

FTIR spectrum of cationic hyperbranched PAMAM-ester is shown in Figure 4.6. The obtained spectrum is found similar to those of hyperbranched PAMAM-ester. When focusing on the region of C=O ester vibration (1728 cm^{-1}), it can be observed that the intensity of C=O ester peak of cationic hyperbranched PAMAM slightly decreases when compared to hyperbranched PAMAM-ester, indicating partial loss of the C=O ester group occurring in the methylation step. In addition, the spectrum of cationic hyperbranched PAMAM-ester shows a broad band at around 3300 cm^{-1} due to the increased number of OH groups. It was likely that part of C=O ester groups was hydrolyzed and converted into COOH group. In deed, FTIR results provide supportive evidence along with elemental analysis to underline that during quaternization step and modification of chitosan, the methyl ester group of cationic hyperbranched PAMAM underwent competitive hydrolysis.

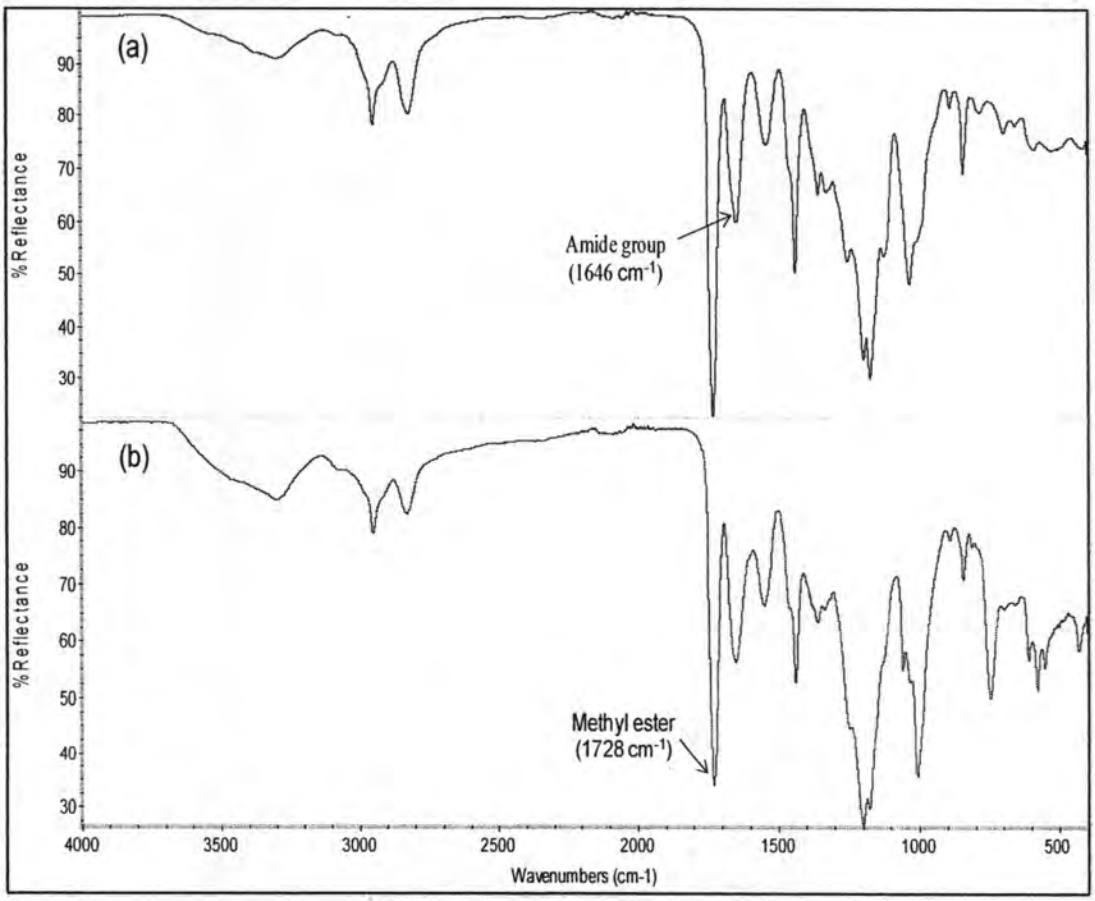

Figure 4.6 FTIR spectra of hyperbranched PAMAM (a) and cationic hyperbranched PAMAM-ester (b)

4.2.2 ^{1}H NMR Analysis

The ^{1}H NMR spectrum of cationic hyberbranched PAMAM G-0.5-ester is shown in Figure 4.7. The signal which is associated to the presence of terminal methyl ester group (CH_3-O-C=O) still strongly appears at 3.61 ppm, indicating that it was intact during methylation step. Following from methylation reaction, the methyl group (CH_3-) was anticipated to be incorporated into tertiary amine, resulting in a quaternary ammonium moiety being introduced into cationic hyperbranched PAMAM-ester as diagrammatically shown in Figure 4.4. It is anticipated that the signal representing methyl proton appears at around 3 ppm in vicinity of methylene proton. As seen in Figure 4.7, it is likely that the strong signal appearing at 3.1 ppm arises from signal overlapping between methyl and methylene protons.

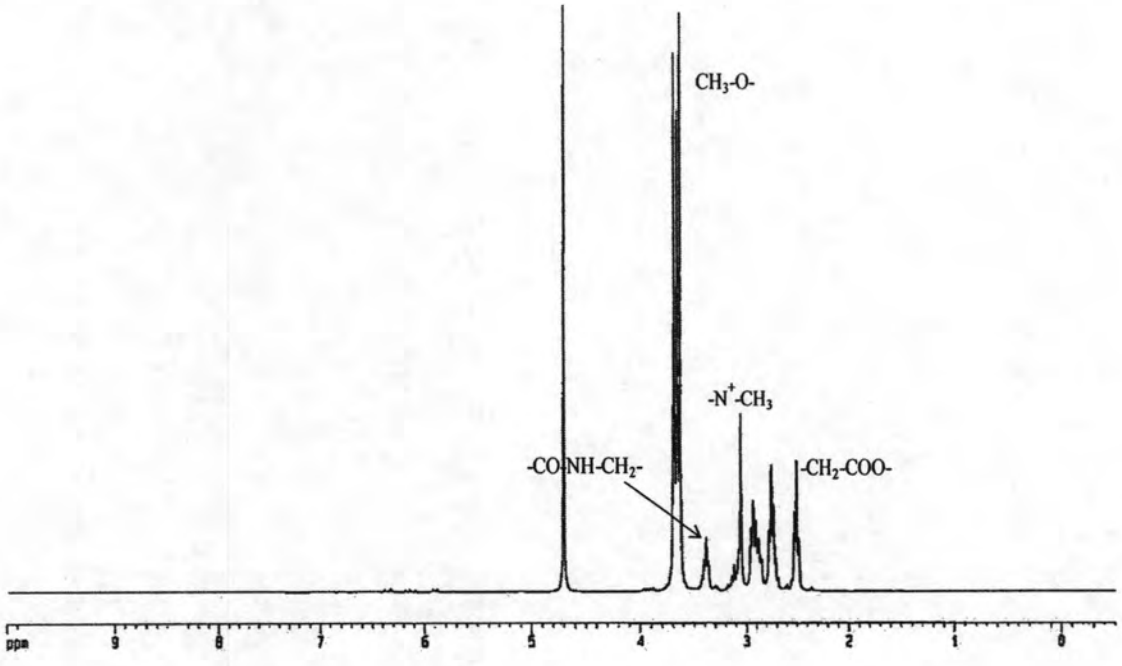

Figure 4.7 ^{1}H NMR spectrum of cationic hyperbranched PAMAM-ester

PART B: MODIFICATION OF CHITOSAN WITH CATIONIC HYPERBRANCHED DENDRITIC POLYAMIDOAMINE

4.3 Modification of chitosan with cationic hyperbranched dendritic polyamidoamine-ester

4.3.1 FTIR Analysis

FTIR spectra of chitosan and cationic hyperbranched dendritic PAMAM-chitosan are presented in Figure 4.8. The spectrum of cationic hyperbranched dendritic PAMAM-chitosan exhibits absorption fingerprint similar to that of chitosan due to their similarity in chemical structure. Despite spectral similarity, the difference in the intensity between chitosan amide band and PAMAM-chitosan amide band at 1640 cm^{-1} is noticeable. As seen, the intensity of PAMAM-chitosan amide band is relatively stronger than the intensity of chitosan amide peak. This indicates that the PAMAM-chitosan has a higher content of amide groups than unmodified chitosan. It is reasonable to say that an increase in the amide band intensity arose from the reaction between chitosan amine group and PAMAM methyl ester group, yielding amide linkage. Based on these evidence, the putative structure of cationic hyperbranched PAMAM-chitosan (excess amount of cationic hyperbranched PAMAM) is proposed as shown in the reaction Figure 4.9. Chitosan modified with excess amount of cationic hyperbranched PAMAM-ester showed a strong intensity of terminal methyl ester group at 1724 cm^{-1} as shown in the reaction Figure 4.8.

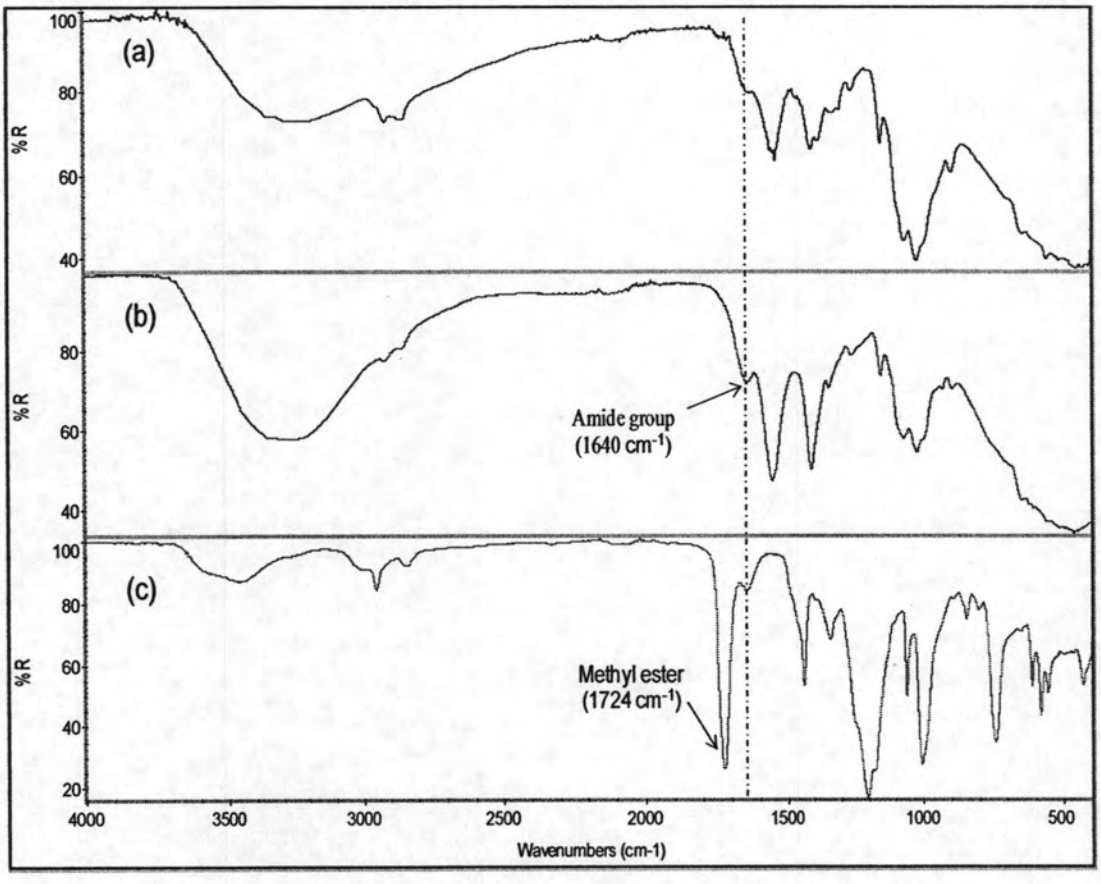

Figure 4.8 FTIR spectra of chitosan (a) and 50 wt% and excessive cationic hyperbranched dendritic PAMAM-chitosan (b and c, respectively)

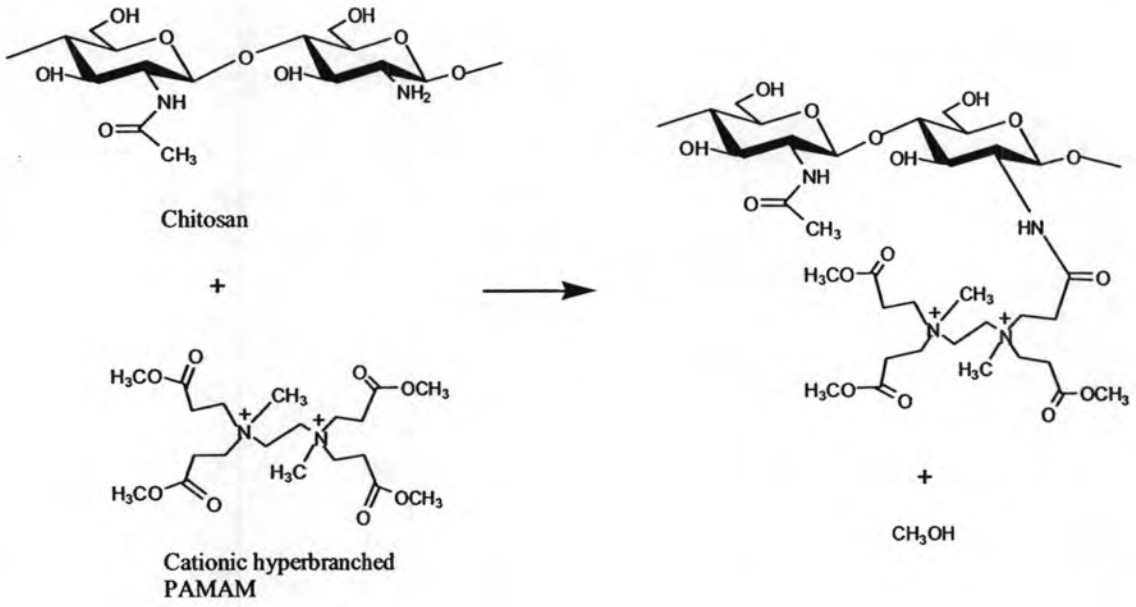

Figure 4.9 Putative structure of cationic hyperbranched PAMAM-chitosan

4.3.2 ^{1}H NMR Analysis

The ^{1}H NMR spectra of chitosan and cationic hyberbranched PAMAM-chitosan are shown in Figure 4.10. The characteristic of chitosan is evidenced by the presence of chemical shifts of chitosan protons at 3.4, 3.2, and 2.6 ppm which are assigned to H3-H6, and H2, respectively. For cationic hyperbranched PAMAM-chitosan, two peak regions are observed between 2.2 and 3.6 ppm, featuring the combination of signals of chitosan protons and hyperbranched PAMAM protons. The signal at 3.1 ppm shows up strongly probably due to the intensity combination of chitosan proton and PAMAM proton. The signal of methyl ester proton at 3.6 ppm totally disappears from the spectra of cationic hyperbranched PAMAM-chitosan, indicating that this group easily underwent reactions including, in this system, amidation with chitosan free amine group and hydrolysis (a side reaction).

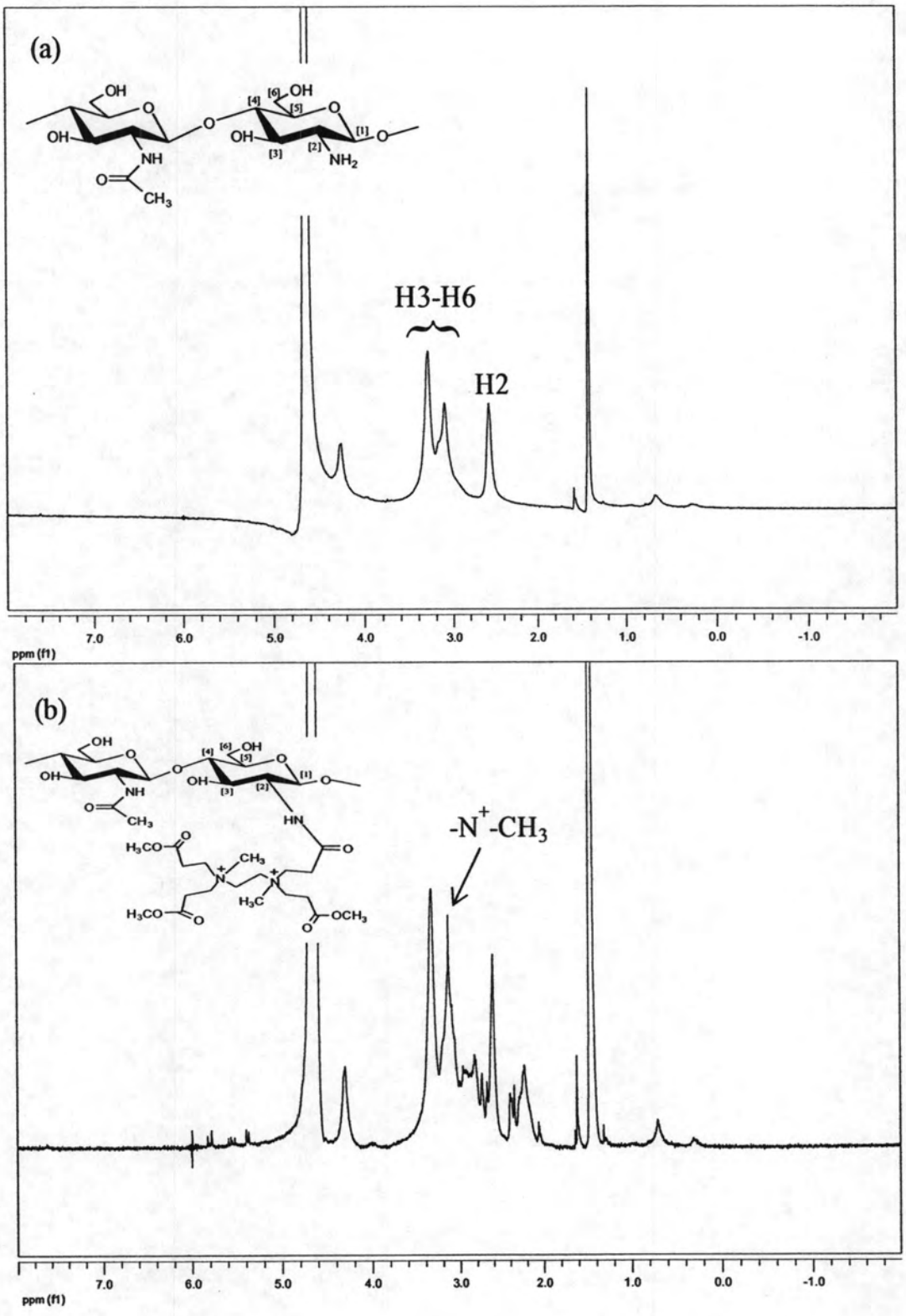

Figure 4.10 ^{1}H NMR spectra of chitosan (a) and cationic hyberbranched PAMAM-chitosan (b)

4.3.3 Elemental Analysis

CHN analysis of modified chitosan was performed. The results from elemental CHN analyzer are presented in Table 4.1.

Table 4.1 Hydrogen (H), carbon (C), and nitrogen (N) percentages (%)

Sample	% C	% H	% N
Chitosan (CTS)	40.20	7.25	7.42
10 wt% PAMAM-CTS	37.55	7.06	7.03
50 wt% PAMAM-CTS	19.77	8.04	3.21
Excessive PAMAM-CTS	33.07	7.12	6.10

The amounts of C and N in the chitosan powder are 40.20 and 7.42 mass %, respectively. The %C and %N found in cationic hyperbranched PAMAM-chitosan are notably lower than chitosan powder whilst the % H of the modified chitosan is found higher than those of virgin chitosan. According to the general appearance, the cationic hyperbranched PAMAM-chitosan is moisture sensitive, resulting in existing in wet cake form. This phenomenon is arising from the presence of bound water due to its moisture sensitivity. In case of chitosan modified with an excess amount of cationic hyperbranched PAMAM, the obtained cationic hyperbranched PAMAM-chitosan is water soluble at neutral pH due to the loosely packed structure and the absence of crosslink. As a matter of fact, the presence of H and O from moisture is associated to the decrease in %C and %N. It was also likely that during the course of methylation reaction the methyl ester terminal groups of the cationic hyperbranched PAMAM could be partially hydrolyzed and converted into the carboxylic acid end groups (-COOH) as proposed in Figure 4.11. As a consequence, the decrease in %C and %N and the increase in %H were partly associated with the additional OH group content.

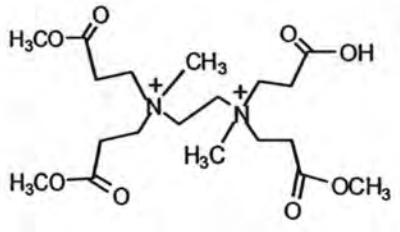

Figure 4.11 Partially hydrolysed product occurring during methylation step

4.3.4 SEM Analysis

Morphology of chitosan and cationic hyperbranched dendritic PAMAM-chitosan films was investigated by a scanning electron microscope. Scanning electron micrographs at 1000x magnification of the surface of the chitosan and cationic hyperbranched dendritic PAMAM-chitosan films are shown in Figure 4.12.

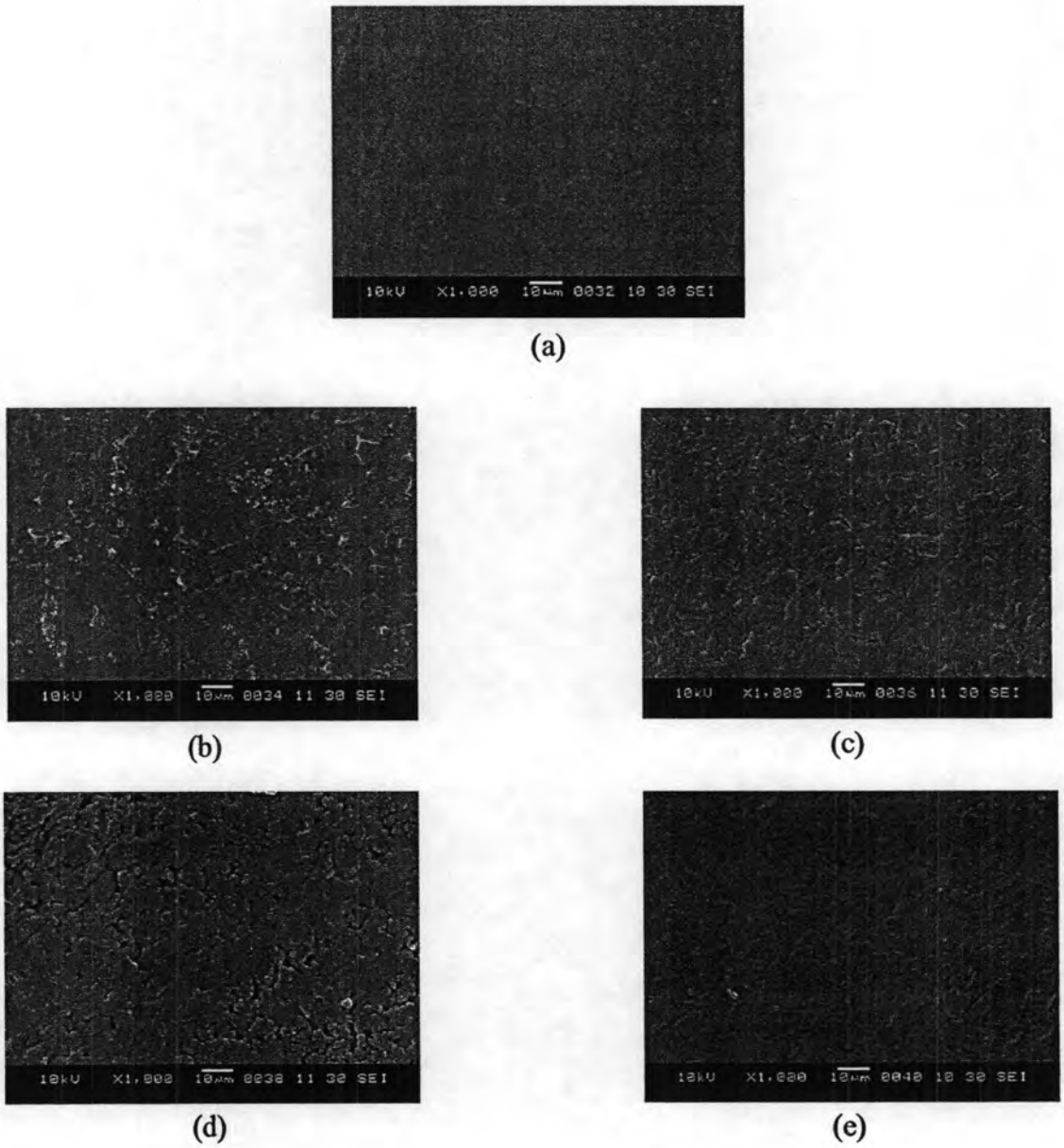

Figure 4.12 SEM photographs of chitosan (a), cationic hyperbranched dendritic PAMAM-chitosan film (10 wt% PAMAM-CTS (b), 50 wt% PAMAM-CTS (c), 100 wt% PAMAM-CTS (d) and 200 wt% PAMAM-CTS (e)

Figure 4.12 (a) shows a relatively smooth, dense and continuous chitosan film without any pores or cracks whereas Figure 4.12 (b) (c) (d) and (e) display the cracking surface of cationic hyperbranched dendritic PAMAM-chitosan films containing 10-200 wt% PAMAM, respectively. As seen, the appearance of cationic hyperbranched dendritic PAMAM-chitosan films is different from virgin chitosan film. Notably, they exhibit rough films with cracks, arising from the characteristic of polymer's weak cohesion. In this case, the cohesion between chitosan polymer chain was interrupted by the introduction of bulky hyperbranched PAMAM into chitosan side chain. As a consequent, flaw crack is obviously evident when compared with virgin chitosan film.

4.3.5 TGA analysis of cationic hyperbranched dendritic PAMAM-chitosan

The TGA thermograms of chitosan, cationic hyperbranched PAMAM and cationic hyperbranched PAMAM-chitosans are shown in Figure 4.13.

The results show that chitosan starts to decompose at above 200 °C with the decomposition peak temperature (Td) of 307 °C whilst cationic hyperbranched PAMAM decomposes more easily at 120 °C with Td of 189°C and 298°C. For cationic hyperbranched PAMAM-chitosan, the mass loss occurs in multiple steps with temperature range of 100-300°C. Upon initial heating, the gradual loss of mass proceeded with Td of 126°C which was believed to be attributable to the loss of bound water followed by the degradation of bonded cationic hyperbranched PAMAM moiety. Further heating resulted in the loss of chitosan backbone with decomposition peak temperature of 287°C. It is seen that the Td of cationic hyperbranched PAMAM-chitosan shifts to relatively lower temperature when compared to pristine chitosan, indicating the lower thermal stability of the modified chitosan. Since the presence of the bulky group (cationic hyperbranched PAMAM moiety) caused an interference with close packing between chitosan molecules it led to an increase in the polymer chain mobility and chain scission.

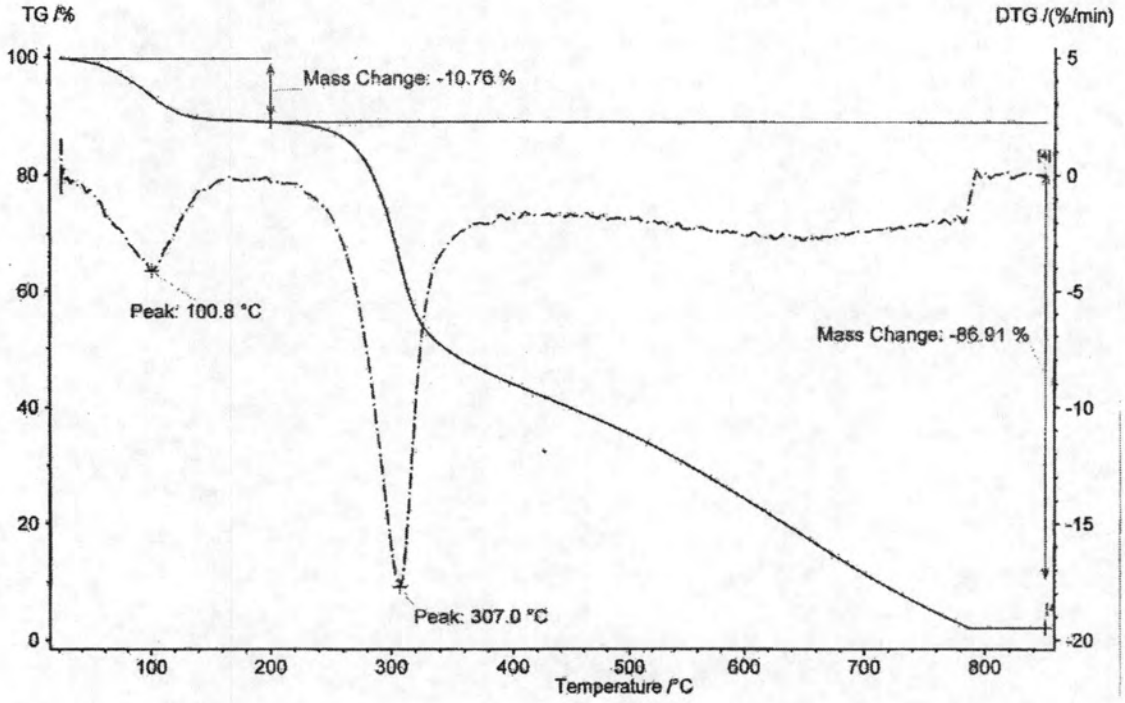
TG /%
DTG /(%/min)
Mass Change: -10.76 %
Peak: 100.8 °C
Mass Change: -86.91 %
Peak: 307.0 °C
Temperature /°C

(a)

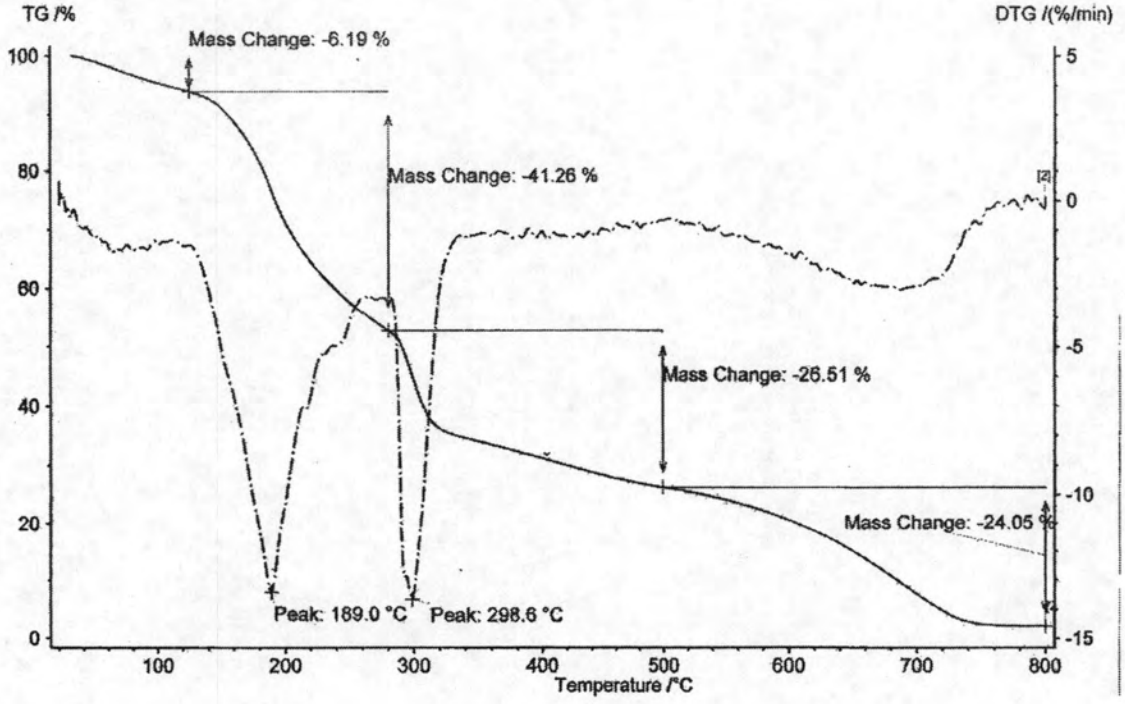
TG /%
DTG /(%/min)
Mass Change: -6.19 %
Mass Change: -41.26 %
Mass Change: -26.51 %
Mass Change: -24.05 %
Peak: 189.0 °C
Peak: 298.6 °C
Temperature /°C

(b)

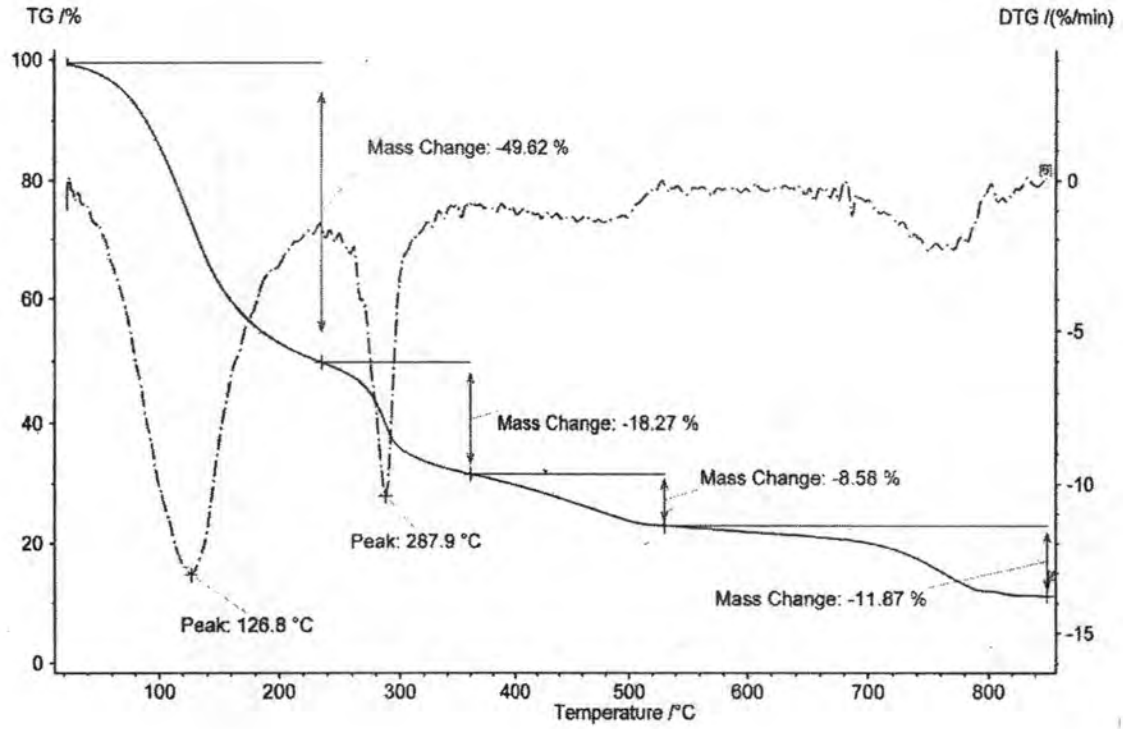

(c)

Figure 4.13 TGA thermograms of chitosan (a), cationic hyperbranched PAMAM (b) and cationic hyperbranched PAMAM-chitosan (c)

4.3.6 X-ray diffraction (XRD)

The XRD diffractograms of film samples including free chitosan and cationic hyperbranched PAMAM-chitosan films are presented. The characteristic of free chitosan film is revealed from the diffractograms illustrated in Figure 4.14. The broad peak found in the region of $2\theta = 15°$ to $30°$ represents the semicrystalline characteristic of a typical chitosan film. As found, the broad peak is observed, indicating that the prepared film exhibits low crystallinity. Chitosan modified with 10 wt%, 50 wt%, and excessive cationic hyperbranched PAMAM was also cast into film for XRD analysis. From Figure 4.14, the modified films containing 10 and 50 wt% cationic hyperbranched PAMAM exhibit similar XRD patterns to those of free chitosan. It is interesting that when the amount of cationic hyperbranched PAMAM

was excessive the resultant modified film was completely amorphous to X-ray diffraction. This phenomenon can be attributed to the fact that an increase in the amount of a bulky group on the chitosan's side chain (cationic hyperbranched PAMAM) leads to an increase in a steric hindrance which directly interferes with crystallization process of chitosan. As a consequence, the chitosan film containing excessive cationic hyperbranched PAMAM is amorphous as evidenced by the total disappearance of semicrystalline peak.

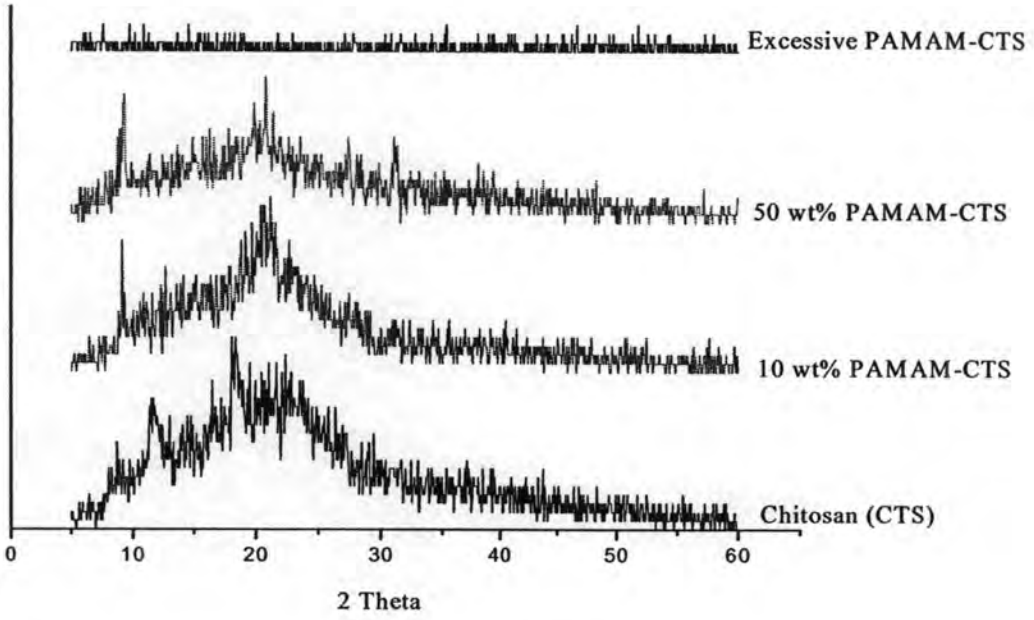

Figure 4.14 XRD diffractograms of chitosan and cationic hyperbranched PAMAM-chitosan films

4.3.7 Antimicrobial activity

The antimicrobial activity of chitosan has been observed against a wide variety of microorganisms, such as, fungi and bacteria. The antimicrobial property is influenced by several factors including the source of chitosan, molecular weight, degree of deacetylation, chemical modification, concentrations, types of microorganism, growth medium and environmental conditions.

In this research, the antimicrobial activity of chitosan and cationic hyperbranched dendritic PAMAM-chitosan films were evaluated by quantitative method. The quantitative test method was carried out to against *Staphylococcus aureus*, the microbial reduction was calculated and presented in Table 4.2.

Table 4.2 The antimicrobial activity of chitosan and cationic hyperbranched dendritic PAMAM-chitosan film

Sample	The number of bacteria CFU/ml (24 hrs.)	% Reduction
Blank	9.7×10^{7}	-
CTS (0.33g)	0	100
50 wt% PAMAM-CTS (0.15g)	1.3×10^{5}	99.86
100 wt% PAMAM-CTS (0.25g) *	1	99.99

* The number of bacteria of blank = 1.3×10^{8}

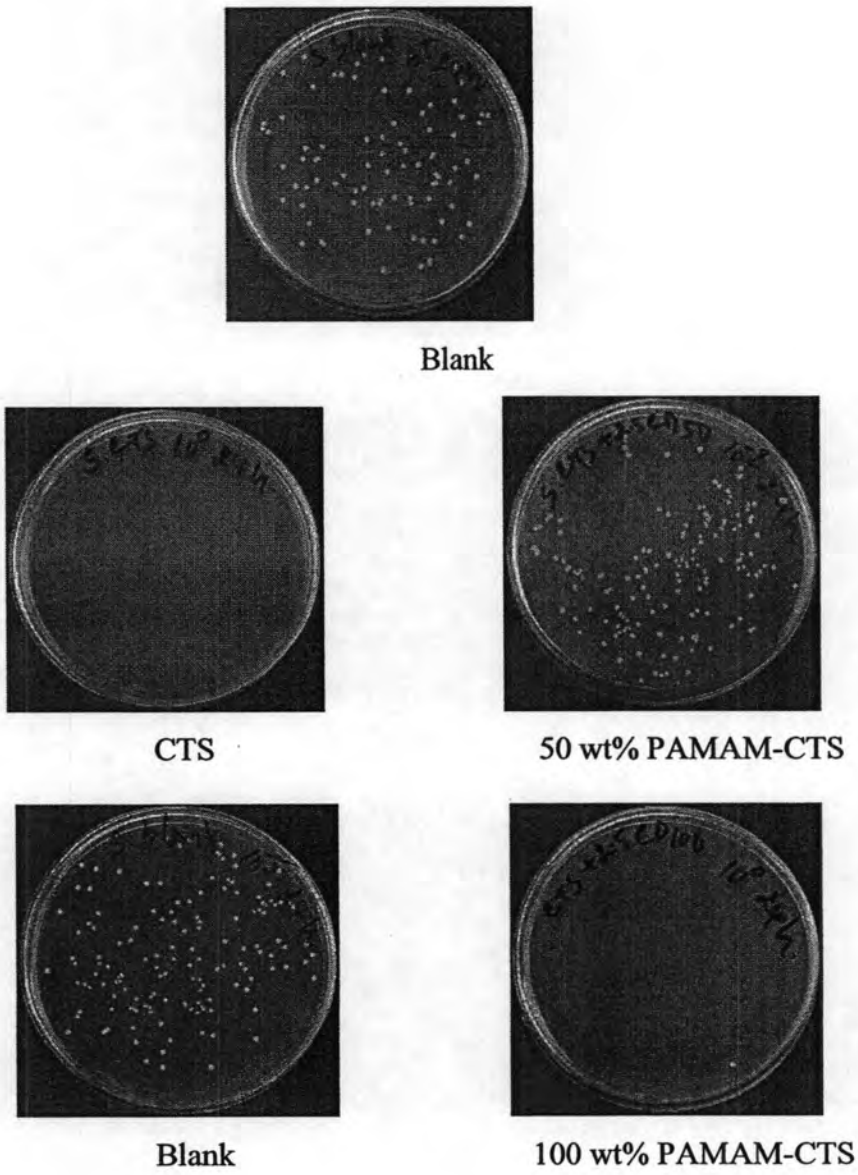

Figure 4.15 Number of bacteria from the blank, CTS, 50 wt% PAMAM-CTS and 100 wt% PAMAM-CTS at 24 hrs. incubation with *Staphylococcus aureus*

Owing to the antimicrobial test method used in this research, the antimicrobial activity is presented in terms of percent microbial reduction. A high percent reduction of bacteria colony indicates an antimicrobial activity of sample.

From Table 4.2, pure chitosan and cationic hyperbranched dendritic PAMAM-chitosan films show excellent antimicrobial activity. It should be note that sample weight of cationic hyperbranched dendritic PAMAM is less than that of pure chitosan weight, namely 0.33 grams chitosan film weight is 0.33 grams when compared to 0.15 grams or 0.25 grams cationic hyperbranched dendritic PAMAM. The results show that cationic hyperbranched dendritic PAMAM-chitosan films exhibit antimicrobial activity against *Staphylococcus aureus* (99.86 and 99.99 percent reduction) which is comparable to pure chitosan film (100 percent reduction). This finding provides information that cationic hyperbranched dendritic PAMAM could additionally enhance antimicrobial performance of chitosan attributable to its cationic character.

In addition, the cationic hyperbranched dendritic PAMAM-chitosan products was left standing in open air to observe antimicrobial behavior. The results after 7 days are shown in Figure 4.16. From the figure, dark spots indicating the presence of fungal spore are apparent in the sample of 10 wt% PAMAM-chitosan. A number of dark spots seem to be less apparent in the samples of 50 and 100 wt% PAMAM-chitosan. In case of the sample of 200 wt% PAMAM-chitosan, no growth of fungi is observed. From this primary observation, it may be assured that cationic hyperbranched dendritic PAMAM-chitosan has ability to inhibit the growth of fungi. It should be point out the the content of cationic hyperbranched dendritic PAMAM plays a role in inhibiting fungi growth.

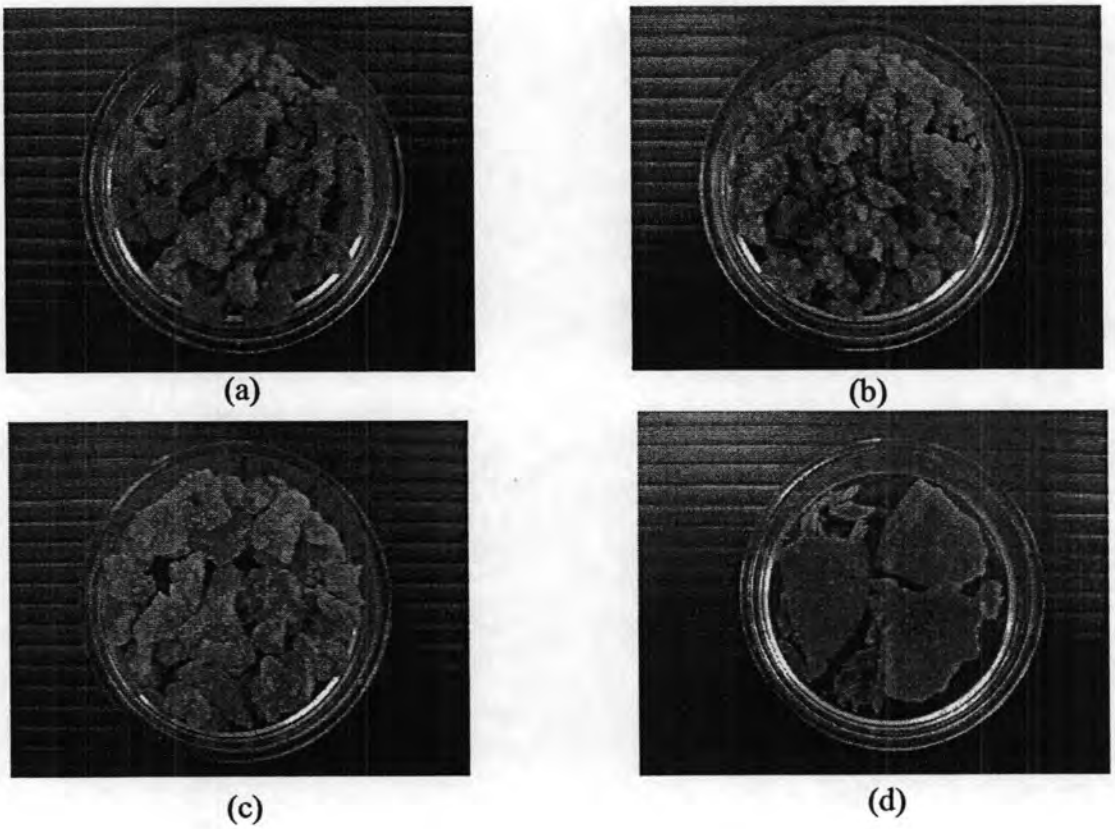

Figure 4.16 Photographs of cationic hyperbranched dendritic PAMAM-chitosan products (10 wt% PAMAM-CTS (a), 50 wt% PAMAM-CTS (b), 100 wt% PAMAM-CTS (c) and 200 wt% PAMAM-CTS (d) after leaving in open air for 7 days

PART C: FABRIC TREATMENT

4.4 Coating of bulk chitosan and in-situ depolymerization of coated chitosan

4.4.1 Antimicrobial activity

The cotton fabric samples were coated with various concentrations of chitosan solution (0.5, 1, 1.5, 2% w/v) and then followed by the depolymerization of coated chitosan with 20 g/l of sodium nitrite for 30 minutes. The laundering test was performed to evaluate the durability of depolymerized chitosan coated on cotton fabric. The washing durability was determined according to ISO 105-C01:1989(E) using a Gyrowash® washing machine, the washing durability test was carried out 1-5 rounds. The fabric samples were determined the antimicrobial properties by quantitative method according to AATCC Test Method 100-1999 (Antibacterial

Finishes on Textile Material). The test was carried out to against *Staphylococcus aureus*. The microbial reduction is presented in Table 4.3 and the photographs of bacterial colonies were shown in Figure 4.17 and 4.18.

Table 4.3 Antimicrobial activity of chitosan coated cotton fabrics, depolymerized fabrics and washed fabrics (2 and 5 cycles)

Sample	The number of bacteria CFU (0 hr.)	The number of bacteria CFU (24 hrs.)	% Reduction
Blank	150	239	-
1% CTS	118	227	0
1% CTS-D	175	269	0
0.5% CTS-D-W2	159	269	0
1% CTS-D-W2	132	234	0
1.5 % CTS-D-W2	131	200	0
2% CTS-D-W2	135	198	0
0.5% CTS-D-W5	132	152	0
1 % CTS-D-W5	137	224	0
1.5 % CTS-D-W5	141	148	0
2 % CTS-D-W5	128	214	0

0.5% CTS-D-W2 = cotton fabric treated with 0.5 % (w/v) chitosan, depolymerization with $NaNO_2$ 20 g/l 30 min. and 2 wash cycles

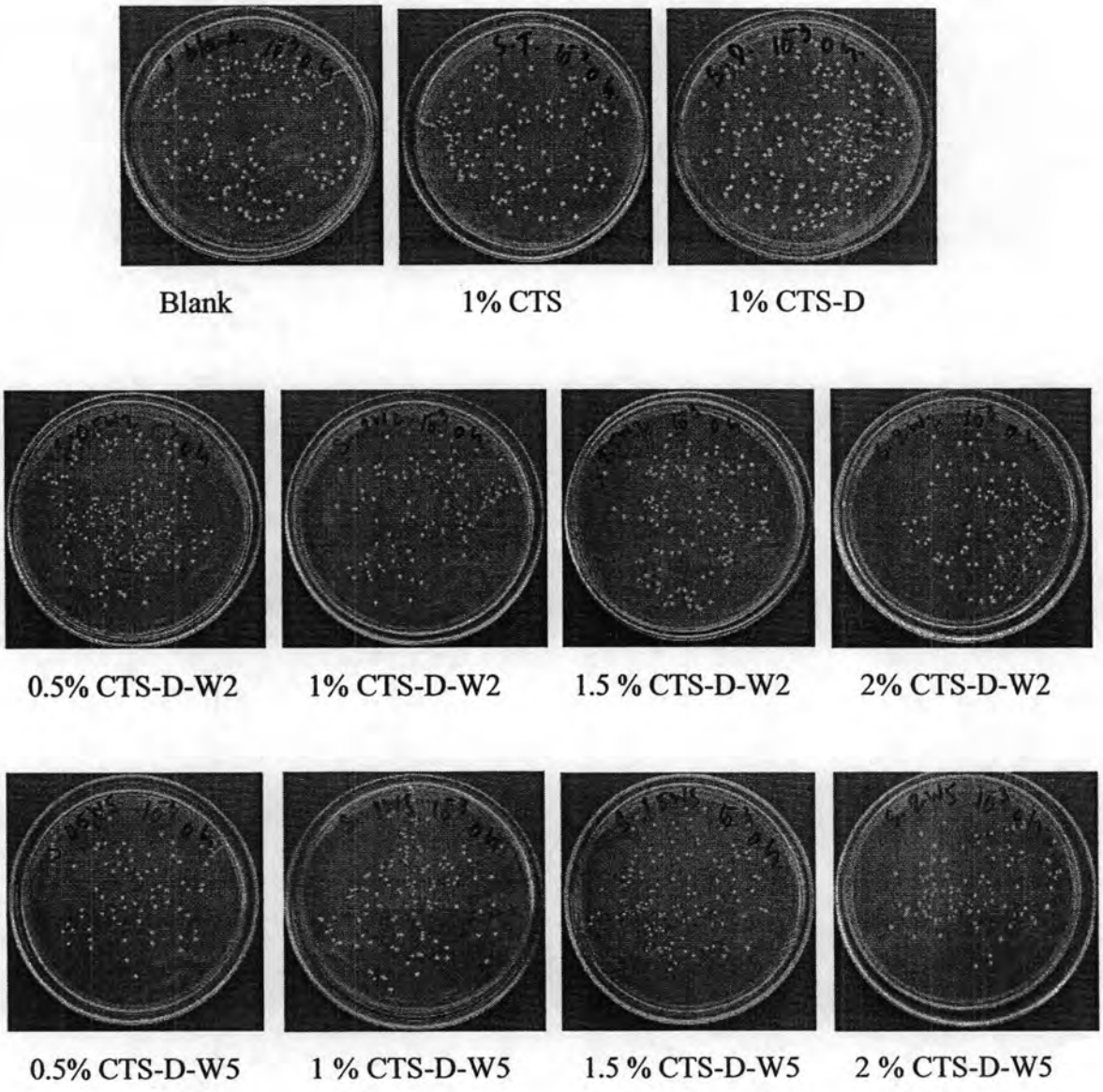

Figure 4.17 Number of bacteria from blank and treated fabric samples at "0" hr. on *Staphylococcus aureus,* incubated at 37°C for 24 hrs.

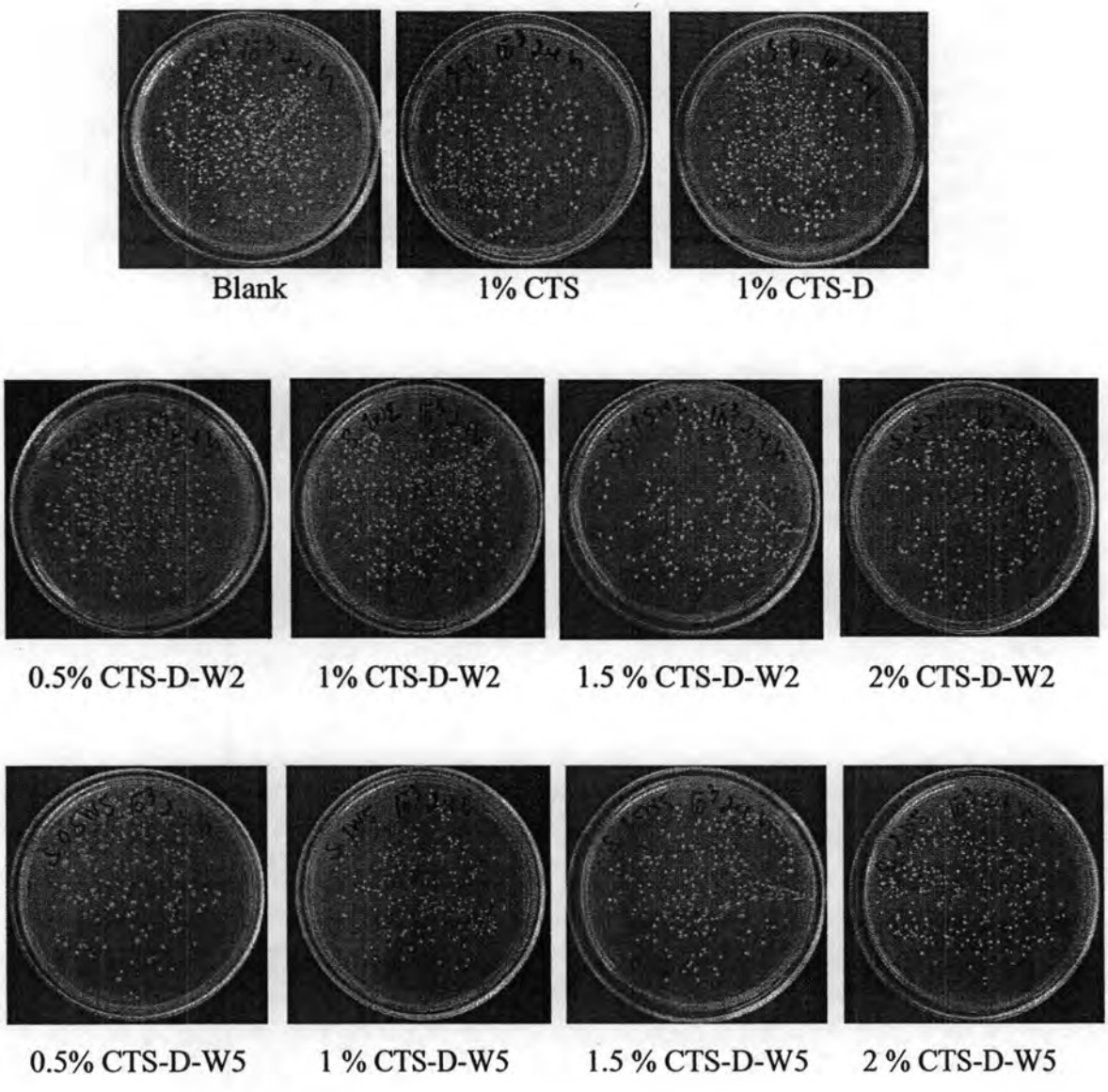

Figure 4.18 Number of bacteria from blank and treated fabric samples at "24" hrs. on *Staphylococcus aureus,* incubated at 37°C for 24 hrs.

The microbial reduction data from Table 4.3 indicates that cotton fabric treated with 1 % w/v chitosan solution shows zero antimicrobial activity. This indicates that chitosan itself was not sufficient to inhibit growth of microorganism. According to SEM images, chitosan film on the fabric surface is found unevenly which probably is responsible for the negative result. In similar manner, the depolymerized chitosan cotton fabrics exhibit zero antimicrobial activity. All washed fabric samples (2 and 5 wash cycles) impressively produce negative result of antimicrobial activity.

4.4.2 SEM Analysis

Morphology of fabric surface was investigated by a scanning electron microscope. Scanning electron photographs at 1000x magnification of the surface of the cotton fabric are shown in Figure 4.16 and those of chitosan treated cotton fabrics and depolymerized chitosan cotton fabrics are shown in Figures 4.19 and 4.20 respectively.

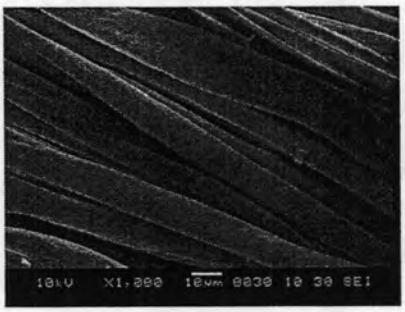

Figure 4.19 SEM photographs of untreated cotton fabric

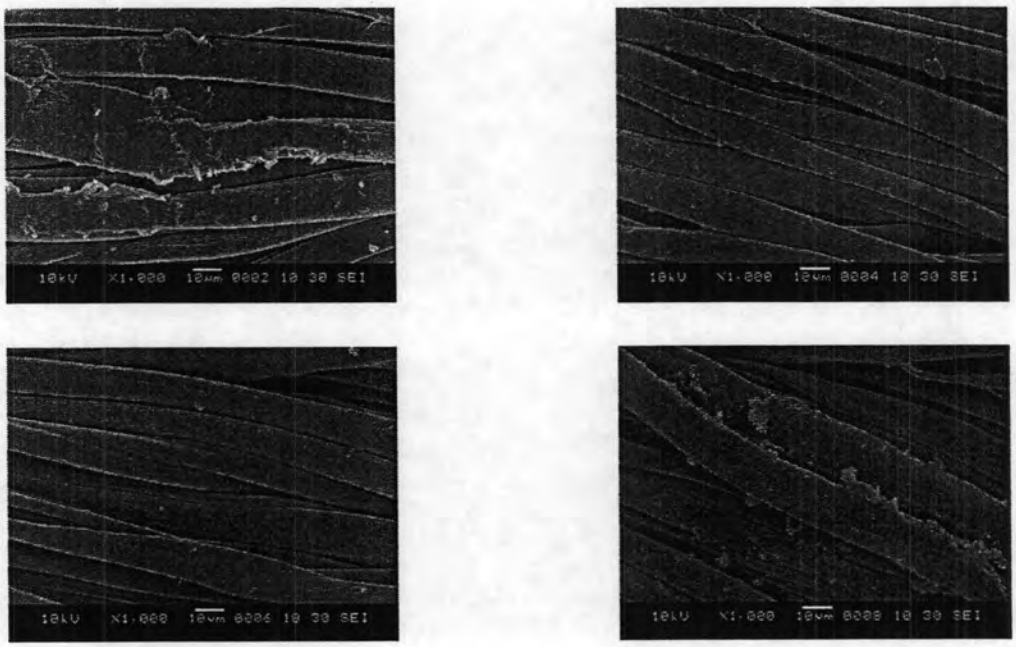

Figure 4.20 SEM photographs of chitosan treated cotton fabrics

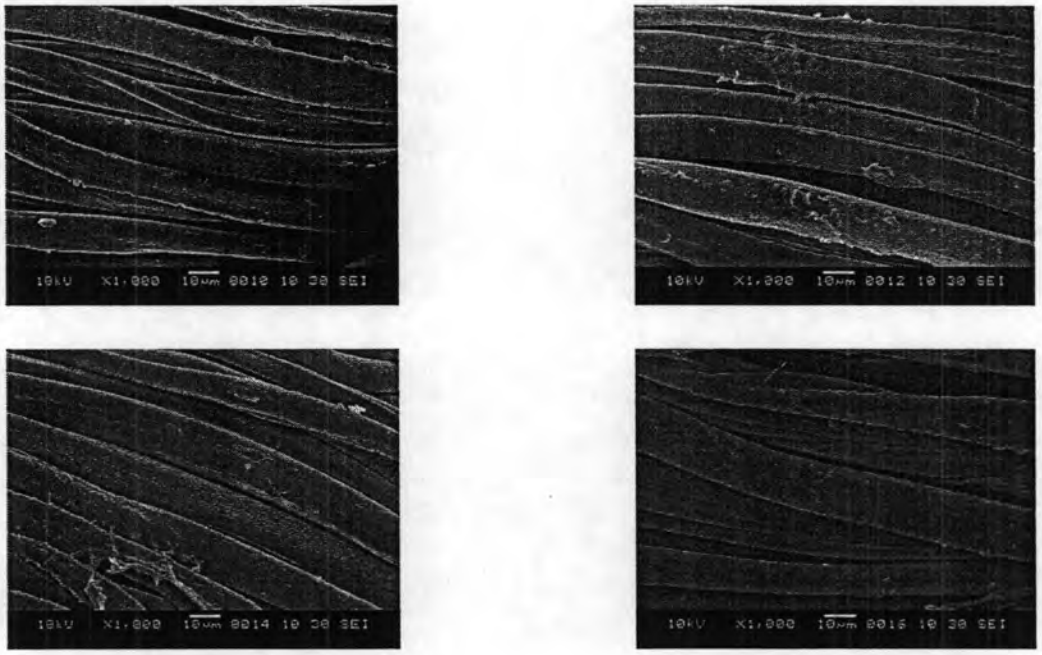

Figure 4.21 SEM photographs of depolymerized chitosan cotton fabric

SEM photographs of chitosan treated cotton fabrics as shown in Figure 4.20 displays chitosan films on the cotton fibers. Figure 4.21 shows the morphology of depolymerized chitosan cotton surface. Figure 4.20 shows that chitosan coating is found predominantly on the surface of cotton. After treatment with sodium nitrite, chitosan residue is still found on the cotton surface, albeit less than chitosan cotton before sodium nitrite treatment. SEM analysis leads to conclude that sodium nitrite treatment could partially remove chitosan coating from cotton surface. Treatment of coated chitosan with sodium nitrite was aimed at coated fabric with an improved stiffness property. Also, its antimicrobial activity was evaluated. As presented earlier, the antimicrobial activity of chitosan coated fabric is not observed.

4.4.3 Nitrogen content analysis

To determine change in the chitosan content due to sodium nitrite treatment, percent nitrogen content was measured by the Kjeldahl method, a method for the quantitative determination of nitrogen. The percent nitrogen found in uncoated fabric, chitosan fabric and sodium nitrite treated chitosan fabric are presented in Table 4.4.

Table 4.4 Nitrogen content of uncoated fabric, chitosan treated fabric and sodium nitrite treated chitosan fabric

Concentration of chitosan solution (%w/v)	% Nitrogen		
	Chitosan treated fabric	Sodium nitrite treated chitosan fabric	2 wash cycles
Control	0.04	-	-
0.5	0.08	0.05	0.04
1	0.13	0.07	0.07
2	0.14	0.13	0.12

The quantitative determination of nitrogen in treated and untreated cotton fabrics was carried out in order to study the alteration of nitrogen content during each process. From table 4.4, it is found that the amount of nitrogen in untreated cotton fabric is 0.04%. In actually, cellulose chain does not possess nitrogen as a composition but in this case the encounter nitrogen may be the impurities in cotton fabric.

Moreover, The amount of nitrogen increase when increase concentration of treating chitosan solution. The nitrogen content in treated fabrics gradually decrease after depolymerization and washing process. It is due to loss of some chitosan content in depolymerization washing process. The result of evaluating nitrogen content is agree with the fabric stiffness report [75].

4.5 Treatment of cationic hyperbranched dendritic polyamidoamine

The cotton fabric samples were treated with aqueous cationic hyperbranched dendritic PAMAM solution (G2.5, G3.5, G4.5) at various concentration (5, 10, 15, 20% w/v) to study antimicrobial activity of treated cotton fabric by a quantitative test method according to AATCC Test Method 100-1999 (Antibacterial Finishes on Textile Material). The test was carried out to against *Staphylococcus aureus*. The microbial reduction is presented in Table 4.5 and the photographs of bacterial colonies were shown in Figure 4.22 and 4.23.

Table 4.5 Antimicrobial activity of cotton fabric treated with cationic hyperbranched dendritic PAMAM

Generation of dendrimer	Dendrimer (% w/v)	% Reduction
2.5	5	77.36
	10	97.87
	15	91.25
	20	90.17
3.5	5	53.70
	10	43.47
	15	57.14
	20	60.37
4.5	5	20.93
	10	38.00
	15	13.88
	20	36.73

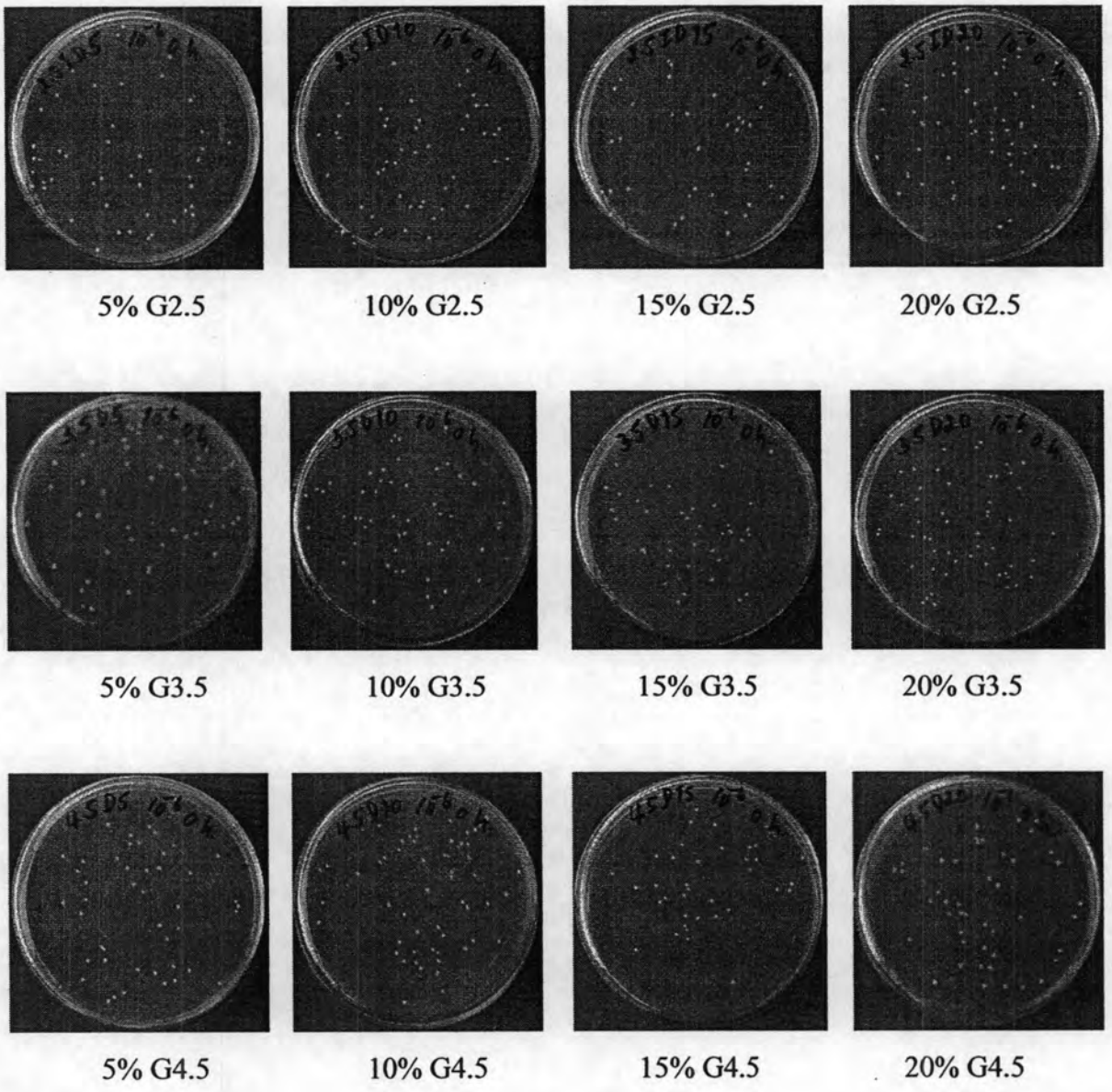

Figure 4.22 Number of bacteria from treated fabric samples at "0" hr. on *Staphylococcus aureus*, incubated at 37°C for 24 hrs.

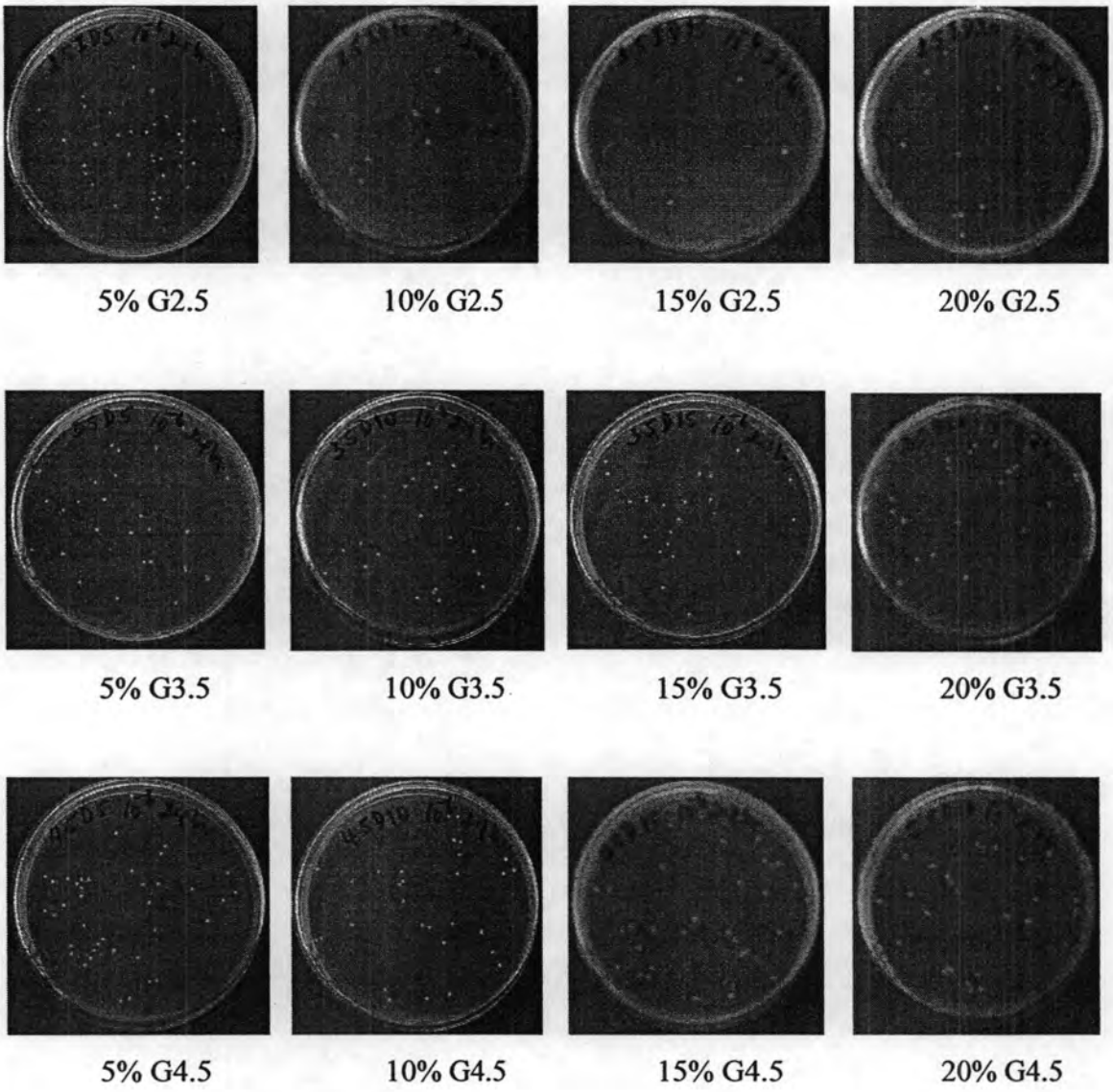

Figure 4.23 Number of bacteria from treated fabric samples at "24" hrs. on *Staphylococcus aureus,* incubated at 37°C for 24 hrs.

The result indicates that cotton fabrics treated with cationic hyperbranched dendritic PAMAM solution have ability to inhibit the growth of *Staphylococcus aureus*. When the generation of cationic hyperbranched dendritic PAMAM increase, its antimicrobial activity decrease. It is likely that as the generation of cationic hyperbranched dendritic PAMAM increased, the bulky terminal groups were prone to hinder the accessibity of dimethyl sulphate into the internal tertiary amine group. As the result, the quaternization sites present in the interior was less susceptible to methylation. Therefore, quaternary ammonium moiety produced in the case of G3.5

and G4.5 was relatively lesser than G2.5. Consequently, their antimicrobial performance is found interior than G2.5 counterpart.

4.6 Combined treatment of cotton fabric with chitosan and cationic hyperbranched dendritic polyamidoamine

4.6.1 Antimicrobial activity

Combined treatment of cotton fabric with chitosan and cationic hyperbranched dendritic polyamidoamine on cotton fabric was carried out for the purpose of studying the synergistic property of treating agent combinations.

First, the cotton fabric samples were treated with a chitosan solution of a various concentrations (0.1, 0.5, 1% w/v) and re-treated with an aqueous cationic hyperbranched PAMAM-ester solution (5, 10, 15, 20% w/v). The treated fabrics were cured at 150 °C to fix chitosan and cationic hyperbranched dendritic polyamidoamine onto cotton fabric.

The antimicrobial activity of treated cotton fabrics was studied by a quantitative test method according to AATCC Test Method 100-1999 (Antibacterial Finishes on Textile Material). The test was carried out to against *Staphylococcus aureus*. The microbial reduction is presented in Table 4.6 and the photographs of bacterial colonies were shown in Figure 4.24 and 4.25.

Table 4.6 Antimicrobial activity of cotton fabric treated with chitosan and cationic hyperbranched dendritic polyamidoamine (combined treatment)

Generation of dendrimer	Dendrimer (% w/v)	Chitosan (% w/v)		
		0.1	0.5	1.0
2.5	15	79.24	76.19	35.0
	20	96.66	97.00	98.75
3.5	15	48.78	7.31	36.84
	20	60.97	62.63	0
4.5	15	58.82	72.72	31.08
	20	44.70	42.25	34.24

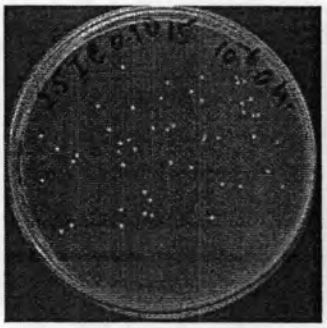

15%G2.5+0.1%CTS

15%G2.5+0.5%CTS

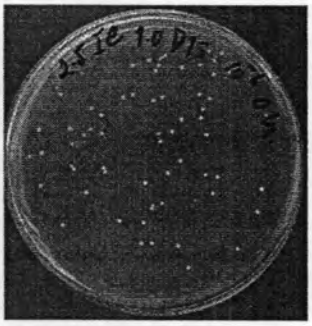

15%G2.5+1.0%CTS

20%G2.5+0.1%CTS

20%G2.5+0.5%CTS

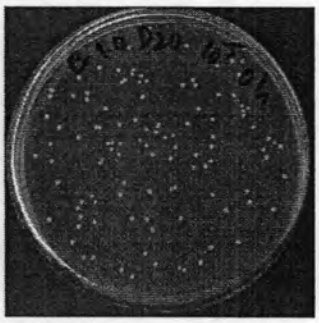

20%G2.5+1.0%CTS

15%G3.5+0.1%CTS

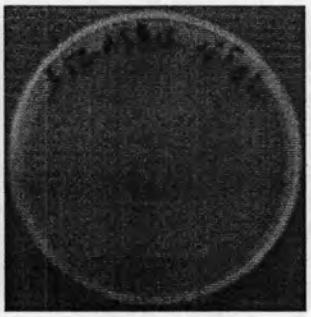

15%G3.5+0.5%CTS

15%G3.5+1.0%CTS

20%G3.5+0.1%CTS

20%G3.5+0.5%CTS

20%G3.5+1.0%CTS

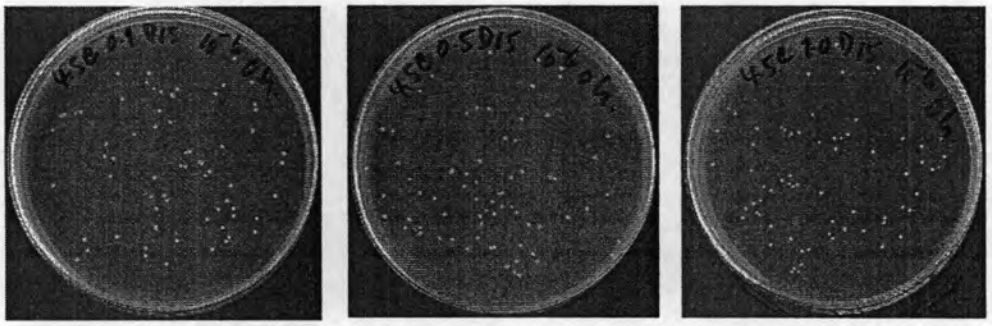

15%G4.5+0.1%CTS 15%G4.5+0.5%CTS 15%G4.5+1.0%CTS

20%G4.5+0.1%CTS 20%G4.5+0.5%CTS 20%G4.5+1.0%CTS

Figure 4.24 Number of bacteria from treated fabric samples at "0" hr. on *Staphylococcus aureus,* incubated at 37°C for 24 hrs.

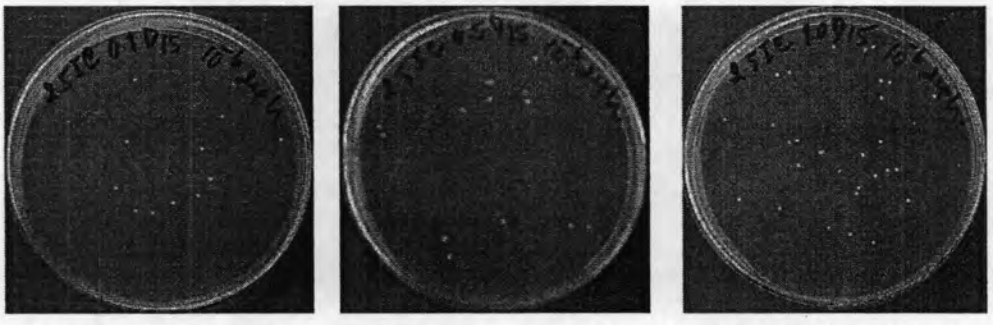

15%G2.5+0.1%CTS 15%G2.5+0.5%CTS 15%G2.5+1.0%CTS

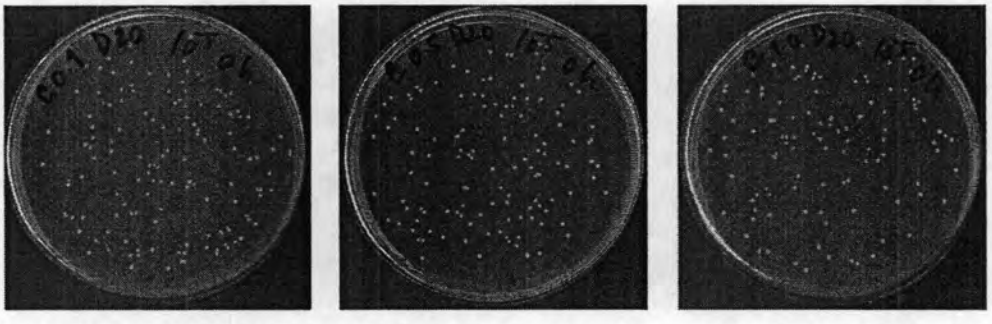

20%G2.5+0.1%CTS 20%G2.5+0.5%CTS 20%G2.5+1.0%CTS

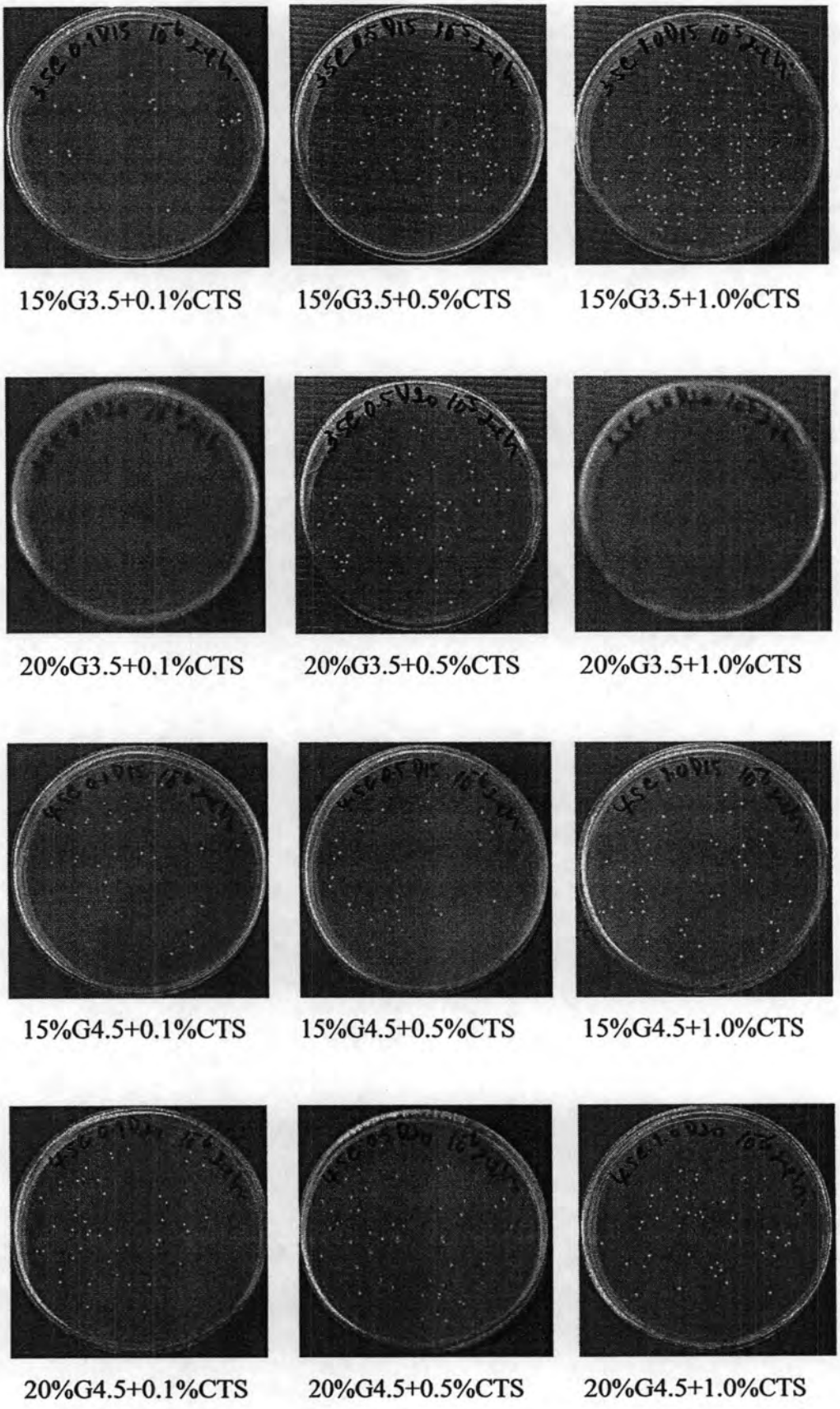

Figure 4.25 Number of bacteria from treated fabric samples at "24" hrs. on *Staphylococcus aureus,* incubated at 37°C for 24 hrs.

From Table 4.7, percent microbial reductions of G2.5 cationic hyperbranched dendritic PAMAM-chitosan cotton fabric exhibit the highest value when compared to G3.5 and G4.5. When chitosan was applied in combination of cationic hyperbranched dendritic polyamidoamine the percent microbial reduction is found insignificantly different. For example, when considering G2.5, the applied chitosan concentrations of 0.1, 0.5, and 1.0 wt % result in the microbial reduction rate of 96.66, 97.0, and 98.75 %, respectively. This indicates that chitosan plays a little role in offering synergistic effect on antimicrobial activity when co-applied with chitosan onto cotton fabric. In case of G3.5 and G4.5 cationic hyperbranched PAMAM, the corresponding antimicrobial activity is found lower than G2.5 cationic hyperbranched PAMAM. The reason was given earlier.

4.6.2 FTIR Analysis

Cotton fabric treated with G2.5 cationic hyperbranched dendritic polyamidoamine and cotton fabric treated with chitosan combined with G2.5 cationic hyperbranched dendritic polyamidoamine were characterized by FTIR analysis. FTIR spectra are presented in Figure 4.26

The spectrum of cotton fabric treated with cationic hyperbranched dendritic PAMAM-chitosan exhibits absorption peak at 1726 cm^{-1}, corresponding to methyl ester group. It can be observed that the intensity of C=O ester peak obtained from cotton fabric treated with chitosan combined with cationic hyperbranched dendritic polyamidoamine diminishes, indicating loss of the C=O ester group. It is due to the fact that the terminated methyl ester groups of cationic hyperbranched dendritic PAMAM-ester was reacted with amine group of chitosan and converted into amide linkage.

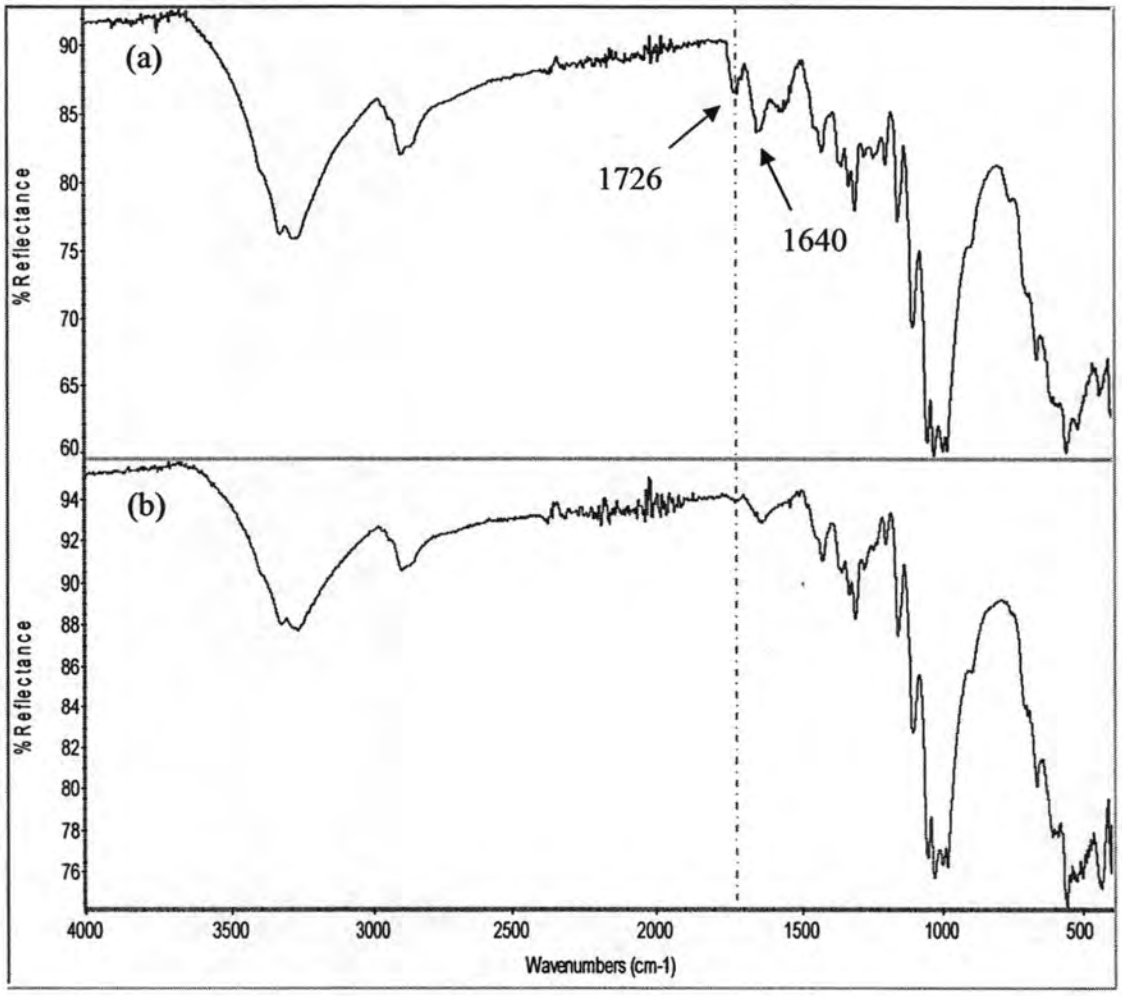

Figure 4.26 FTIR spectra of cotton fabric treated with G2.5 cationic hyperbranched dendritic polyamidoamine (a) and cotton fabric treated with chitosan and G2.5 cationic hyperbranched dendritic polyamidoamine (b)

4.6.3 SEM Analysis

The surface morphology of fabric was investigated by a scanning electron microscope. Scanning electron photographs at 1000x magnification of the fabric surface of the cotton fabric and cotton fabrics treated with chitosan and cationic hyperbranched dendritic polyamidoamine by combined treatment is shown in Figure 4.27.

SEM photograph of the untreated cotton fabric shows a smooth fibers's surface (top) while those of cotton fabrics treated with chitosan combined with cationic hyperbranched dendritic polyamidoamine (bottom) display chitosan/ cationic hyperbranched dendritic polyamidoamine films on the cotton fibers.

Figure 4.27 SEM photographs of untreated cotton fabric (top) and cotton fabrics treated with chitosan combined with cationic hyperbranched dendritic polyamidoamine (bottom)